

A novel concept of combined cold expansion and surface processing of fastener holes using rotating tool

Nitin J. Panaskar

A Dissertation Submitted to
Indian Institute of Technology Hyderabad
In Partial Fulfillment of the Requirements for
The Degree of Master of Technology



भारतीय प्रौद्योगिकी संस्थान हैदराबाद
Indian Institute of Technology Hyderabad

Department of Mechanical Engineering

June, 2013

Declaration

I declare that this written submission represents my ideas in my own words, and where others' ideas or words have been included, I have adequately cited and referenced the original sources. I also declare that I have adhered to all principles of academic honesty and integrity and have not misrepresented or fabricated or falsified any idea/data/fact/source in my submission. I understand that any violation of the above will be a cause for disciplinary action by the Institute and can also evoke penal action from the sources that have thus not been properly cited, or from whom proper permission has not been taken when needed.




(Signature)

Nitin Panaskar

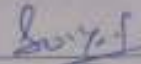
ME11M10

Approval Sheet

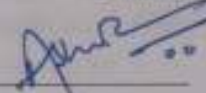
This thesis entitled – Novel concept of combined cold expansion and nanocomposite surface layering of fastener holes using rotating tool – by – Nitin Panaskar – is approved for the degree of Master of Technology from IIT Hyderabad.




Dr A. Venugopal Rao
DMRL (DRDO), Hyderabad
Examiner



Dr. S Surya Kumar
Department of Mechanical Engineering
IIT Hyderabad
Adviser
Examiner



Dr. Abhij Sharma,
Department of Mechanical Engineering
IIT Hyderabad
Adviser



Dr. Chandra Shekhar Sharma,
Department of Chemical Engineering
IIT Hyderabad
Chairman

Acknowledgements

With immense pleasure I express my deep and sincere gratitude, regards and thanks to my thesis advisor, **Dr. Abhay Sharma** for his excellent guidance, invaluable suggestions and continuous encouragement at all the stages of my research work. His wide knowledge and logical way of thinking have been of great value for me. As a guide he has a great influence on me, both as a person and as a professional. I am able to complete my project successfully with his support.

I would like to thank **Prof. U. B. Desai** Director of IIT Hyderabad and **Prof. Vinayaka Eswaran** HOD for Department of Mechanical Engineering for approving this project and guiding, encouraging me all through the course of the project.

It was a great pleasure to me as a part of Department of Mechanical, IIT Hyderabad and I would like to thank all the staff members and my friends for helping me in all stages of my work and making the great place to work in.

I would also like to thank my batchmates and M.Tech friends **Bhoopati, Robin and Naresh** for their moral support and sharing of knowledge which has been helpful to me so far. A special thanks goes to PhD scholars **Nilanjan** and **Srilakshmi** for providing me support in my project work. I would like to thank **Moulali Syed, Dhananjay Sahoo, A.Pravin and Jagdish** for helping me in the Work shop. Being with friends in IIT Hyderabad was a nice experience which will be the most memorable part of my entire life. The days I have spent in IIT H has been very nurturing and invaluable to me.

Above all, I extend my deepest gratitude to **my parents** for their invaluable love, affection, encouragement and support.

Dedicated to

My Parents

&

My Sisters

Abstract

Bolts, rivets and location pins are commonly used in various engineering applications for assembly of components and structures. The holes produced for the assembly is susceptible to cracks due to fatigue caused by tensile loads applied. These cracks can be prevented or its propagation can be prolonged by inducing compressive residual stress in the material around the hole. Cold expansion hole is one of the techniques used to induce compressive stress zone, by inserting a tapered mandrel/pin or ball into an undersized hole. A novel application of the cold expansion and surface modification of walls of the cylindrical hole is presented. Pre-drilled holes of different diameters in commercially available aluminum and Al-2014-T6 aluminum alloy plates are cold expanded using a specially fabricated tapered tool that rotates and simultaneously traverses through the hole. The tapered tool expands the hole to the desired diameter and also stirs the internal wall of the hole. In order to understand the role of frictional heating and stirring in the cold expansion of holes three mediums, namely, dry (without cooling and lubricating), metal working fluid (cooling and lubricating) and Al_2O_3 nanoparticles (lubricating and frictional heating) are used. The residual stress, surface roughness and hardness of the wall of the holes are measured and SEM images are captured. Significant residual stresses are induced in the material around the hole region. Significant hardness improvement with reasonable surface finish is obtained. Moreover the cold expanded holes showed considerable improvement in the fatigue life of the holes. The fatigue life is found to be directly proportional to residual stresses induced around the hole and inversely proportional to surface roughness. Hardness has a negative impact on fatigue life. The rotating tool cold expansion process is compared with conventional cold expansion process and good efficiency of cold expansion is achieved in case of Al-2014-T6 aluminum alloy material using nanoparticles, in terms of fatigue life achieved. It is observed that frictional heating and the plastic deformation have combined effect on the performance of the cold expansion of cylindrical holes.

Nomenclature

Symbol	Description	Unit
σ	Residual stress	N/mm ²
F	Force	N
F _h	Force in lateral/horizontal direction	N
F _z	Force in axial/vertical direction	N
Θ	Angle of tilt	Degrees

Contents

Declaration.....	ii
Approval Sheet	iii
Acknowledgements.....	iv
Abstract.....	vi
Nomenclature	vii
1 Introduction	1
2 Background	5
2.1 Conventional cold working.....	5
2.2 Cold expansion methods	6
2.2.1 Ball expansion method	6
2.2.2 Tapered pin/ Mandrel method	7
2.2.3 Split mandrel method	8
2.2.4 Split mandrel with sleeve method	9
2.2.5 Roller burnishing method.....	11
2.2.6 Torsion and cols expansion method	12
2.2.7 Spherical mandrelling method.....	12
2.3 Gaps and opportunity.....	13
2.4 Problem Definition, Objective and Scope.....	14
3 Material and Experimental method	16
3.1 Process description.....	16
3.2 Material.....	17
3.3 Tools	18
3.4 Machine and experimental set-up	18
3.5 Experimental method.....	20
3.6 Measurement and Tests.....	21
3.6.1 Residual stress	21
3.6.2 Surface roughness and topography.....	21
3.6.3 Ovality.....	21
3.6.4 Hardness	22
3.6.5 Surface Texture	23
3.6.6 Fatigue life.....	23

4 Results and Discussion	24
4.1 Part A : Pure Aluminium	24
4.1.1 Residual stress	24
4.1.2 Surface roughness.....	29
4.1.3 Surface topography.....	30
4.1.4 Ovality.....	34
4.1.5 Hardness	34
4.1.6 Surface Texture	35
4.1.7 Fatigue life.....	37
4.1.7.1 Effect of residual stress on fatigue Life.....	38
4.1.7.2 Effect of surface roughness on fatigue Life.....	40
4.1.7.3 Effect of hardness on fatigue Life	43
4.2 Part B : Al Alloy (Al-2014 T6).....	44
4.2.1 Residual stress	44
4.2.2 Surface roughness.....	45
4.2.3 Surface topography.....	46
4.2.4 Ovality.....	49
4.2.5 Hardness	50
4.2.6 Surface Texture	51
4.2.7 Fatigue life.....	53
4.2.7.1 Effect of residual stress on fatigue Life.....	54
4.2.7.2 Effect of surface roughness on fatigue Life.....	55
4.2.7.3 Effect of hardness on fatigue Life	58
5 Conclusion and Future work	60
5.1 Conclusions.....	60
5.2 Scope of future work.....	61
References	62
Appendix	65

List of Figures	Page No.
1. An Aircraft structure	1
2. Residual stress profile around a cold expanded hole	2
3. Cold expansion tool and work piece	3
4. Ball cold expansion	7
5. Tapered pin cold expansion	7
6. Split Mandrel Method	8
7. Split Sleeve Method	10
8. Roller Burnishing Tool Image	11
9. Schematic representation of local torsion.....	12
10. Spherical mandrelling method	13
11. RTCE Tool.....	18
12. Image of the set-up.....	19
13. Image of the fixture for RTCE under nano condition	19
14. Image of the fixture for RTCE under dry conditions	19
15. Image of the fixture for RTCE under wet condition	20
16. Process flow – (a) Drilling, (b) Cold expansion, (c) Burnishing	20
17. Image of the X-Ray diffraction machine.....	22
18. Measurement positions for ovality showing periphery of the hole.....	22
19. Fatigue Test Sample	23
20. Load vs Time graph for constant amplitude sine load	24
21. Fatigue Life Testing	24
22. Graph of residual stress for various DCE for RTCE.....	26
23. Graph of residual stress distribution for nano RTCE with burnishing for various DCE.....	26
24. Graph of axial force (Fz) vs. time for nano RTCE for various DCE	27

25. Graph of lateral force (Fh) vs. time for nano RTCE for various DCE.....	27
26. Graph of residual stress distribution for 5.26 % DCE for nano RTCE with burnishing	28
27. Graph of residual stress for RTCE with and without burnishing for 5.26% DCE	28
28. Graph of surface roughness for Ra values for RTCE at 5.26% DCE	29
29. Graph of surface roughness for Rz values for RTCE at 5.26% DCE	30
30. Surface topography under Dry conditions for RTCE at 5.26 % DCE without burnishing	31
31. Surface topography under Dry conditions for RTCE at 5.26 % DCE with burnishing	31
32. Surface topography under Wet conditions for RTCE at 5.26 % DCE without burnishing	32
33. Surface topography under Wet conditions for RTCE at 5.26 % at DCE with burnishing	32
34. Surface topography under Nano conditions for RTCE at 5.26 % DCE without burnishing	33
35. Surface topography under Nano conditions for RTCE at 5.26 % DCE with and without burnishing	33
36. Ovality measurement for RTCE at 5.26% DCE	34
37. Hardness measurement for RTCE at 5.26% DCE	35
38. SEM image showing texture of cylindrical wall for CCE at 5.26 % DCE	35
39. SEM images showing texture of cylindrical wall for various conditions of (a) Wet RTCE without Burnishing, (b) Wet RTCE With Burnishing, (c) Dry RTCE without Burnishing, (d) Dry RTCE With Burnishing, (e) Nano RTCE without Burnishing, (f) Nano RTCE With Burnishing for Aluminium material at 5.26% DCE.....	36
40. Graph of Fatigue Life for RTCE at 5.26% DCE.....	37
41. Comparison of Fatigue Life with Residual stress for RTCE at 5.26% DCE and CCE specimens	38

42. Conventional cold expansion set-up.....	39
43. Tapered tool used for conventional cold expansion.....	39
44. Graph of Fatigue life and Residual stress comparison for RTCE at 5.26% DCE and CCE.....	40
45. Graph of Fatigue life and Surface roughness (Ra) comparison for RTCE at 5.26% DCE without burnishing.....	41
46. Graph of Fatigue life and Surface roughness (Ra) comparison for RTCE at 5.26% DCE with burnishing.....	41
47. Graph of Fatigue life and Surface roughness (Rz) comparison for RTCE at 5.26% DCE without burnishing.....	42
48. Graph of Fatigue life and Surface roughness (Rz) comparison for RTCE at 5.26% DCE with burnishing.....	42
49. Graph of Fatigue life and Hardness comparison for RTCE at 5.26% DCE without burnishing	43
50. Fatigue life and Hardness comparison for RTCE with burnishing at 5.26% DCE	44
51. Graph of residual stress for RTCE at 5.26% DCE for three conditions with and without burnishing	45
52. Graph of surface roughness for Ra values for RTCE at 5.26% DCE	46
53. Graph of surface roughness for Rz values for RTCE at 5.26% DCE	46
54. Graph of Surface topography under Dry conditions for RTCE at 5.26 % DCE without burnishing	47
55. Graph of Surface topography under Dry conditions for RTCE at 5.26 % DCE with burnishing	47
56. Graph of Surface topography under Wet conditions for RTCE at 5.26 % DCE without burnishing	48
57. Graph of Surface topography under Wet conditions for RTCE at 5.26 % DCE with burnishing	48
58. Graph of Surface topography under Nano conditions for RTCE at 5.26% DCE without burnishing	49
59. Graph of Surface topography under Nano conditions for RTCE at 5.26 % DCE with burnishing	49

60. Graph of Ovality measurement for RTCE at 5.26 % DCE.....	50
61. Graph of Hardness measurement for RTCE at 5.26 % DCE.....	51
62. SEM images showing texture of cylindrical wall for various conditions of (a) CCE, (b) Wet RTCE without Burnishing, (c) Wet RTCE With Burnishing, (d) Dry RTCE without Burnishing, (e) Dry RTCE With Burnishing, (f) Nano RTCE without Burnishing, (g) Nano RTCE With Burnishing for Al-2014 T6 material at 5.26% DCE.....	51
63. SEM image showing texture of cylindrical wall for CCE at 5.26% DCE	52
64. Graph of Fatigue Life for RTCE at 5.26% DCE.....	54
65. Graph of Fatigue Life comparison with Residual stress for RTCE at 5.26% DCE	54
66. Fatigue life and Residual stress comparison of RTCE at 5.26% DCE and CCE specimens.....	55
67. Graph of Fatigue life and Surface roughness (Ra) comparison for RTCE at 5.26% DCE without burnishing.....	56
68. Graph of Fatigue life and Surface roughness (Ra) comparison for RTCE at 5.26% DCE with burnishing.....	56
69. Graph of Fatigue life and Surface roughness (Rz) comparison for RTCE at 5.26% DCE without burnishing.....	57
70. Graph of Fatigue life and Surface roughness (Rz) comparison for RTCE at 5.26% DCE with burnishing.....	57
71. Graph of Fatigue life and Hardness comparison for RTCE at 5.26% DCE without burnishing	58
72. Fatigue life and Hardness comparison for RTCE with burnishing at 5.26% DCE	59

List of Tables

Page No.

1. Mechanical properties of material used.....	17
2. Chemical composition of material used	18
3. Fatigue life of RTCE operated specimens (Al).....	37
4. Fatigue life of RTCE operated specimens (Al-2014 T6)	53

Chapter 1

Introduction

Bolts, rivets and location pins are widely used for connecting components, especially in the aerospace industry. Rivets are the most widely used mechanical fasteners especially in aircraft fuselage structures. Hundreds of thousands of rivets are utilized in the construction and assembly of a large aircraft. Solid rivet with universal head is one of the most widely used rivet type in aircraft fuselage manufacturing and repairing processes. The presence of holes in the in-service components can lead to high tensile stress concentration around these holes. The stress concentration around these holes is significant and the applied cyclic tensile loads can lead to fatigue failure of the structure. As per statistical data, fatigue failure of the fastener holes account for 50-90 % of fracture of aircrafts and the surface finish of the holes have direct effect on reliability and usage. The anti-effect of stress concentration can be reduced and the fatigue life can be improved by introducing a compressive stress field around the material of the hole [1–5].

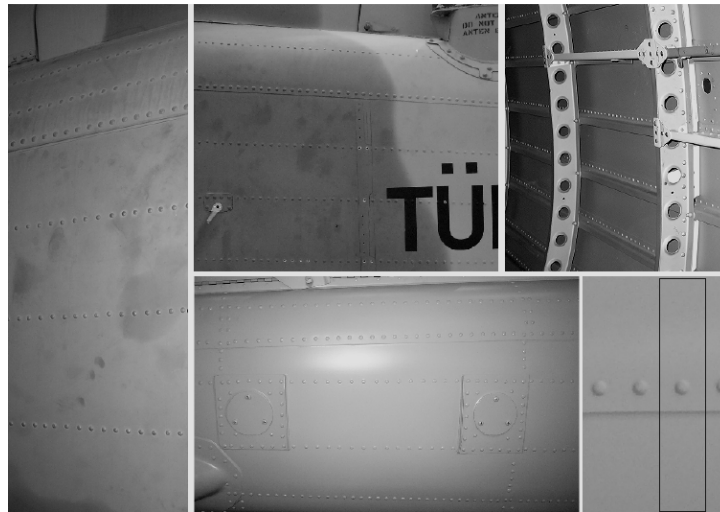


Figure 1 : An aircraft structure [6]

Cold expansion process has been commonly used to improve the fatigue life (usually 3-5 times) of fastener holes since past 40 years [7]. This process was developed by Boeing company and is presently being marketed by Fatigue Technology Inc. (FTI). The basic process of cold expansion involves insertion of an oversized ball or tapered pin or mandrel from one side (entry face) of the hole and removing it from the other side (exit face). When the mandrel is removed, the elastically deformed material springs back from its expanded state and also leads to the material in the elasto-plastic region to contract. This results in the accumulation of compressive residual stresses in the plastic zone around the region of the hole. These compressive stresses delay the initiation and propagation of fatigue cracks.

The region nearest to the hole has compressive residual stresses increase to a maximum value at a specific distance away from the hole. This region is known as the reverse yielding zone. The initial drop in compressive residual stresses is due to the reversal of strain direction of the material which in turn has occurred due to the spring back of the material after the cold expansion process. This phenomenon is also known as the Bauschinger effect. After reaching the maximum compressive stress value, the residual stresses drop down and finally become tensile in nature. The residual stresses are thus self-equilibrating in nature. This stress field is also known as self-stress field. The residual stress profile of a cold expanded hole is shown in fig. 2.

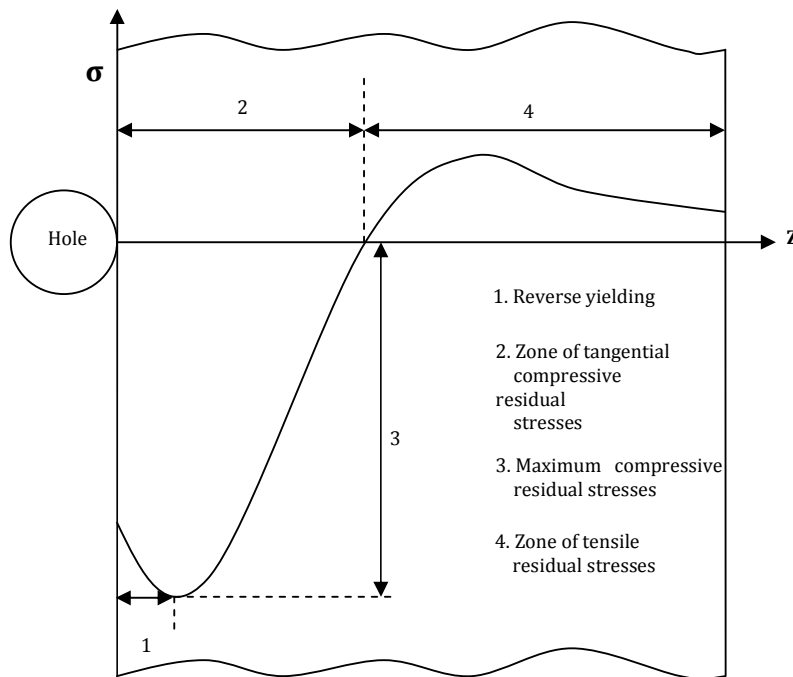


Figure 2 : Residual stress profile around a cold expanded hole

Benefits of Cold expansion :

1. Crack growth rate is reduced.
2. Reduces maintenance costs by preventing unscheduled maintenance and the time intervals between inspections are increased.
3. Repair of in-service components is possible.
4. Increased product utility due to aircraft readiness.

Another method involves using a lubricating solid or split sleeve to avoid direct contact with the cold expanded surface and thereby prevent surface damage[7]. The effect of the tapered rotating tool without sleeve has been investigated in the present study.

In the present study, a tapered rotating tool is used with a specific feed to cold expand the hole as shown in fig. 3. The combined effect of stirring and the mechanical pressure applied by the rotating tool on the inner surface of the hole in the presence of nano-sized particles may produce a nanocomposite layer along the inner surface of the hole, thereby resulting in grain refinement and enhanced hardness of the hole surface.

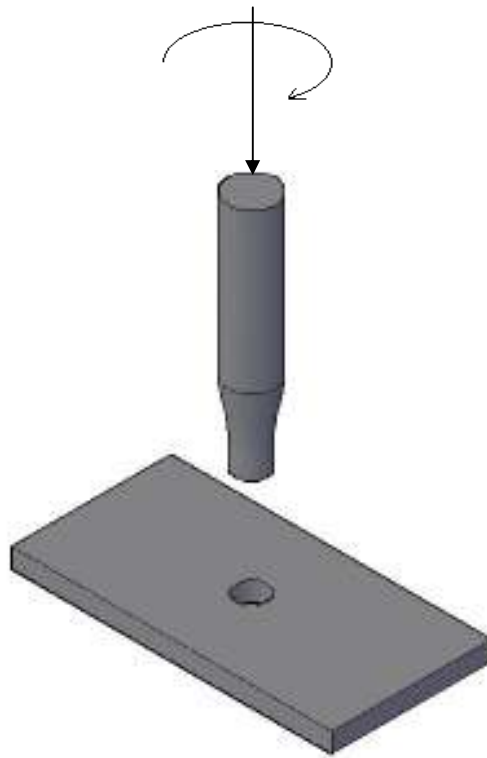


Figure 3 : Cold expansion tool and work piece

The process can also be carried out using metal working fluid as a cooling and lubricating medium as well as in dry condition. The nanocomposite layer formed may not be uniform across the along the surface of the hole. This can lead to higher degree of surface roughness which can affect the fatigue life of the component. Therefore the cold expansion operation is performed followed by the burnishing operation which will press the nanocomposite layer uniformly on the surface and produce a smooth and hard surface. Moreover, the drilling, cold expansion and burnishing operations should be done subsequently without altering the position of the work piece to get the best results. The present study is supposed to be the first one which investigates the possibility of producing cold expansion and nanocomposite layering in a single process. This will take combined advantage of the beneficial compressive stresses obtained from cold expansion process and the strengthening effect of the grain refinement obtained from the stirring action.

The implementation of friction due to tool rotation changes the profile of the residual stresses induced by the cold expansion. This implies a significant interaction between the two processes, i.e. cold expansion and stirring, with respect to the residual stresses and hardness distribution around the fastener hole. The process is termed as rotating tool cold expansion (RTCE).

The subsequent chapters include :

‘Background’ describes the various cold working and cold expansion, the existing gaps and opportunities and the definition, objective and scope of the problem.

‘Material and Experimental method’ describes the process, the materials and tools used, machine set-up, experimental methods and the measurement techniques used for rotating tool cold expansion process.

‘Results and discussion’ discusses about the effects of surface finish, residual stress and hardness on the fatigue life of rotating tool cold expanded (RTCE) holes. Also discusses the results obtained for RTCE carried out using various mediums and at various degrees of cold expansion.

Finally this report is concluded in chapter titled ‘Conclusions’ with the recommendations for future work

Chapter 2

Background

Cold working operation has been carried out since last 50 years to induce residual stresses in the material. Various methods of cold working such as shot peening, stress coining, autofrettaging and mandrelizing, also known as cold expansion, are being used in industry. Cold expansion is popular method of cold working used to induce residual stresses around the region of the hole. Various methods of cold expansion such as ball expansion method, tapered pin/mandrel method, split mandrel method, split mandrel with sleeve method, roller burnishing method torsion and cold expansion method and spherical mandrelling method are used. The following section gives a brief description on the various cold working and cold expansion methods.

2.1. Conventional Cold working can be done using different methods as below :

1. Shot Peening

Shot peening is a process in where round metallic, glass or ceramic particles are impinged on the surface so as to relieve the tensile stresses in the surface or induce compressive residual stresses. This operation is used for springs, aerospace automotive applications to increase the fatigue life of the components.

2. Stress coining

Stress coining process uses a tool with a serrated pole stem. There are protuberances on the tool with smaller diameter protuberances near the tip of the tool and the diameter of the protuberances increases farther from the tool tip. The tool can be attached to a gun. The rapid force vibration of the tool impacts through the hole and is then retracted back similarly.

3. Autofrettaging

Autofrettaging is a technique in which pressure is used which yields the inner portion of the component plastically and the deeper portion is deformed elastically. After the pressure is relieved, the elastically deformed areas tend to return to their original state while the plastically deformed areas tend to prevent this action. This results in the formation of internal compressive stresses near the inner surface of the component. This method is commonly used in the manufacturing of pressure vessels, rail cross borings, canon barrels, oil and gas wells etc.

4. Using interference fit pressure: Mandrelizing

Various processes such as solid mandrel cold expansion, split mandrel cold expansion and split sleeve cold expansion use interference fit pressure on the surface of the hole to cause cold expansion of the hole.

2.2. Cold Expansion Methods

2.2.1. Ball expansion method

The ball expansion method as shown in fig. 4. is one of the oldest methods of cold expansion. The contact of the ball with the surface can damage the surface finish. Hence the ball cold expansion operation is generally followed by a reaming operation. Amrouchea et. al [8] carried out numerical simulations to display the influence of DCE on the distribution of equivalent stresses around the hole during the process of the cold expansion. They used ball cold expansion for aluminium alloy (Al 6082-T6) and steel using pre-cracked specimen. Gopalakrishna et al. [9] compared tapered mandrel technique with the ball technique using a 4 mm thick plate of Al 2024 alloy.

The former method produced 200 % more fatigue life as compared to latter. The fatigue life improved up to 5 % DCE beyond which it decreased. It was also observed that the effectiveness of the taper pin method was more significant at higher levels of cold expansion as the amount of difference in the fatigue life increases.

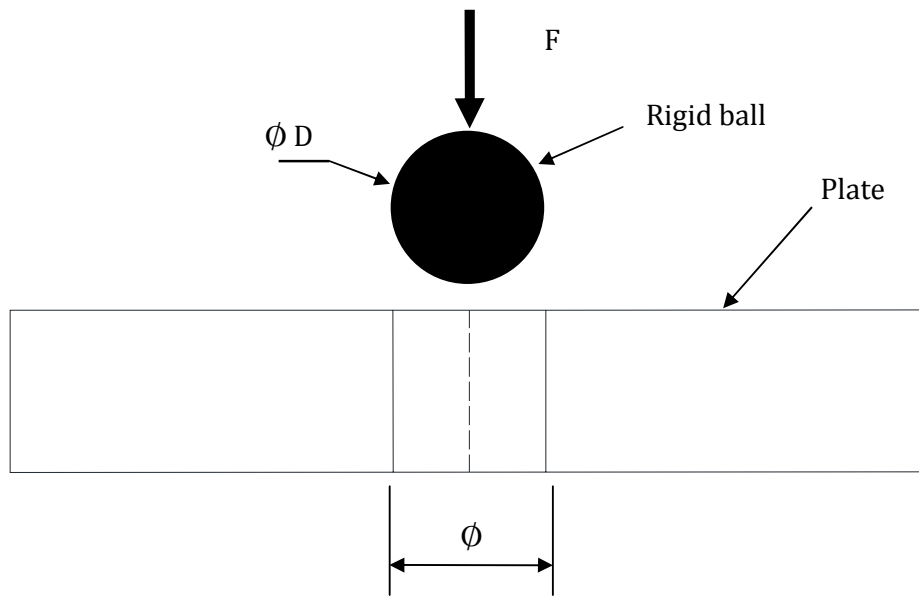


Figure 4 : Ball cold expansion

2.2.2. Tapered pin/mandrel method

The tapered pin method is studied as it is a basic type of cold expansion and does not involve the complexities of sleeve during FEM simulation. The direct contact between the pin and hole results may damage the hole surface. The tapered pin/ mandrel method is shown in fig. 5.

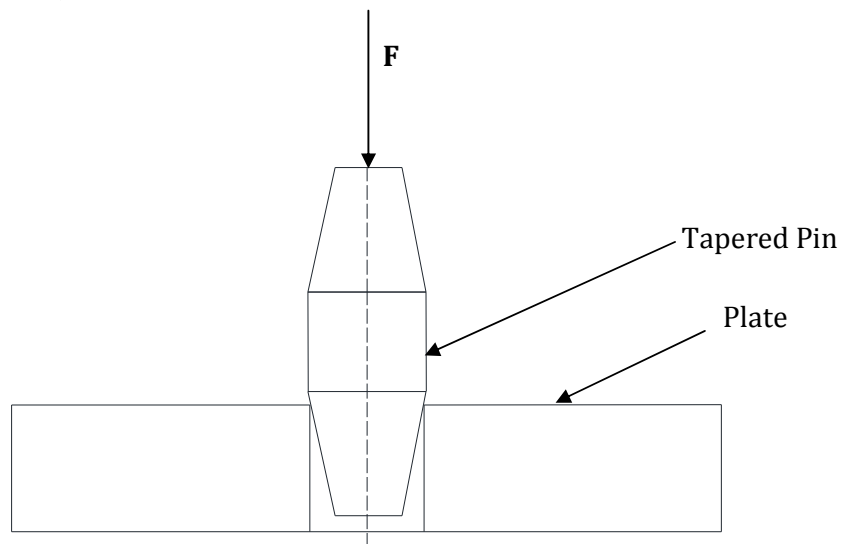


Figure 5 : Tapered pin cold expansion

Farhangdoost et al. [10] simulated the effect of different mandrel speeds on residual stress using finite element method in case of 2A12T4 and observed that increase in mandrel speed results in an increase in residual stress distribution. These findings were verified by experimental data. Chakherlou et al. [11] used a tapered pin for cold expansion of 6.32 mm plates Al 7075-T6. They observed that the maximum compressive stresses occur at the hole edge near the midplane. The fatigue life is higher at low alternating stress than at high alternating stress. Chakherlou et al.[12] used a pre-lubricated to study cold expansion of Al 2024-T3 in double shear lap joints and observed that larger cold expansion size usually leads to better fatigue life when using 0%, 1.5% and 4.7% DCE. The positive effect of cold expansion in case of double shear lap joint is considerably lower compared to the single plate. J. Liu et al.[13] performed cold expansion of 2A1₂T₄ plate of 4 mm thickness using a tapered mandrel and observed that compressive residual stress at the entrance face is not uniform along the layer depth. The fatigue life of the cold expanded hole improved 6 folds for 6 % degree of cold expansion (DCE). It was also observed that the fatigue crack of the cold expanded holes always initiates on entrance face.

2.2.3. Split mandrel method

The split mandrel with sleeve is used to develop a prescribed amount of plastic deformation around the hole. When the mandrel is removed, a residual stress field is created in the region surrounding the hole. In split mandrel, the mandrel itself can collapse to enable its insertion in the hole during the start of the cold expansion process. This is achieved by longitudinally slotting the tapered mandrel into quarters. The split mandrel method is shown in fig. 6.

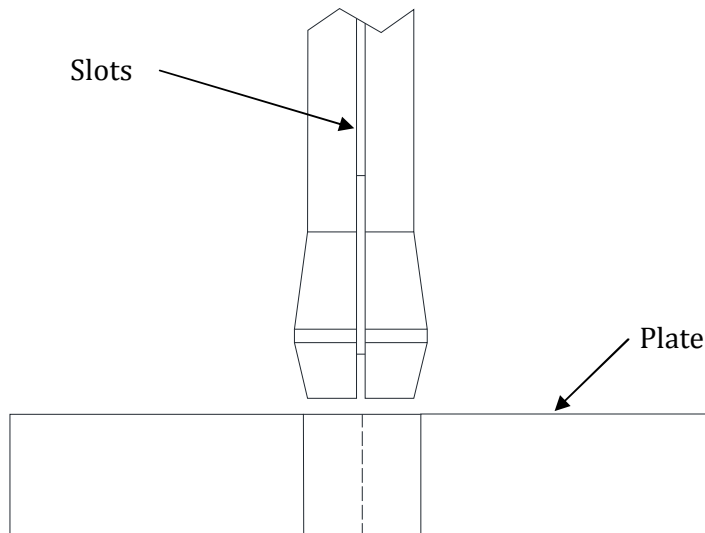


Figure 6 : Split Mandrel Method

2.2.4. Split mandrel with sleeve method

In split sleeve, the sleeve used is collapsible and gets detached from the mandrel after cold expansion, as shown in fig. 7. This operation is also followed by a reaming operation. The split sleeve mechanism is used most widely [9]. The lubricated split sleeve allows for single-sided processing. The split is placed over the mandrel and this combination is used for cold expansion. After the cold expansion operation, the sleeve is removed and discarded. The force required to pull back the mandrel is considerably reduced and the hole surface does not have to undergo the large axial frictional forces generated when the mandrel is drawn out. The split-sleeve method creates an axial ridge which corresponds to the position of the split, which can be removed by reaming. However, this causes the residual compressive stresses to develop asymmetrically, with lower hoop stresses in the vicinity of the split. Also there is possibility of shear cracks occurring at the axial ridge. These effects of these cracks cannot be eliminated completely but can be reduced by giving maximum reaming allowance. This may possibly reduce the fatigue enhancement benefits of cold expansion. The process used by FTI uses a split sleeve mandrel.

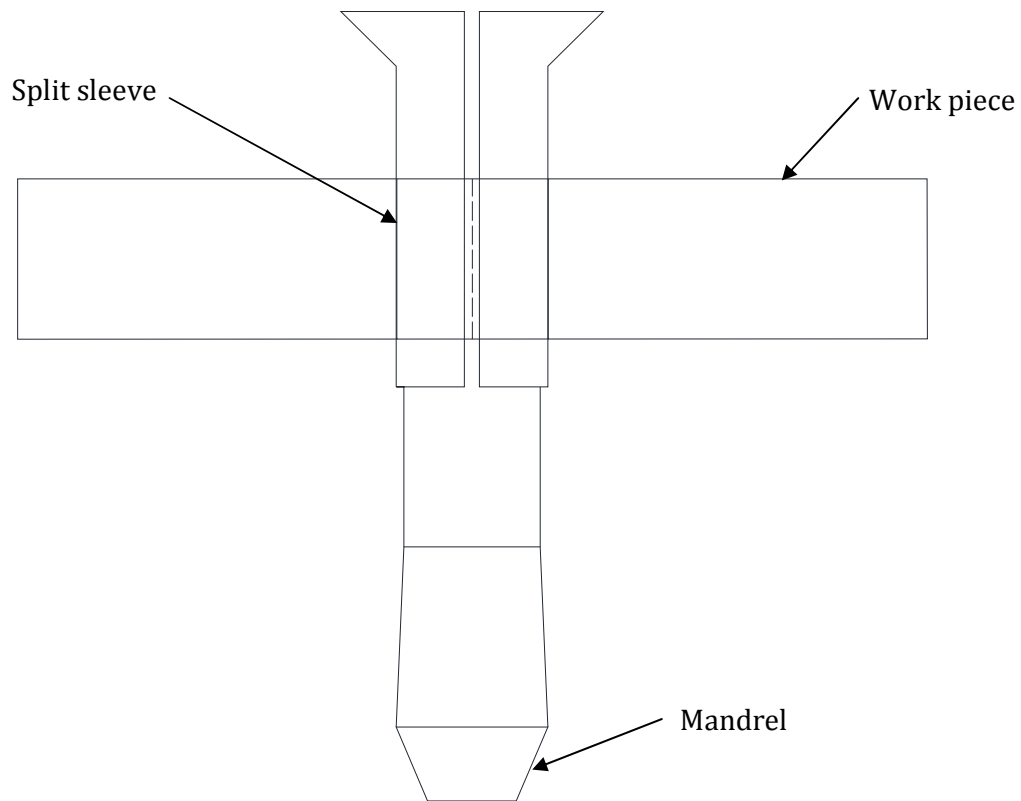


Figure 7 : Split Sleeve Method

Yongshou et al. [14] studied the effects of friction between the mandrel and the hole's surface using both split sleeve and split mandrel process. The effect of friction was found to be local and affects only the residual stresses around the maximum value and near the hole edge. Observation which found in other studies, that in cold expanded holes, crack always initiates near entrance face was confirmed. It was also find that the crack propagates faster along the transverse direction than along the axial direction.

Burlat et al. [15] used a split sleeve tool to perform cold expansion on Al7475-T7351 plates of 6.35 mm plate thickness. They observed that the life improvement factor (LIF is ratio of 'total life of cold expanded hole' to 'total life of non cold expanded hole') increases as the DCE is increased up to 5.58% and this factor is more prominent at low stress than at high stress.

Yan et al. [16] conducted cold expansion on titanium TC4 specimens.. They found that the fatigue life of cold expanded holes are increased 1.5-3 times as compared to that of 'as drilled' holes. It was noticed that in case of cold expanded hole, crack always initiates from the entrance surface, while for the "as drilled" hole, it initiates from the mid-plane of the hole.

Matos et al. [17] performed cold expansion on a 5 mm hole predrilled in a Alclad 2024-T3 aluminium alloy plate of thickness 2 mm. Compressive residual stresses were induced around the hole region. The residual stresses at the exit face were found to be higher than those at the entry face. The fatigue behavior of aeronautical structures is studied using open-hole specimens in Al-alloy 2024-T3, with and without hole expansion.

2.2.5. Roller burnishing method

Roller burnishing is a cold working method used to induce compressive residual stresses and enhance surface finish in metals. The tool typically consists of a tapered mandrel and cylindrical rollers held in a cage. The tool moves with a specified feed rate and rotational speed. The rollers are pressed on the part being processed, thereby, producing a very consistent finish across the part. Although, the use of roller burnishing is limited in the context of cold expansion, it is very popular as a surface finishing technique. The roller burnishing tool is shown in fig. 8.



Figure 8 : Roller Burnishing Tool Image

Ozdemir et al. [18] compared split sleeve and roller burnishing methods of cold expansion. In roller burnishing cold expansion, there is plastic flow of material along the thickness of the hole, due to which there is some reduction in the overall compressive stresses induced by cold expansion. The sleeve on the contrary prohibits any such transverse motion. Thus, the split sleeve method gives better fatigue life as compared to roller burnishing. However, the combined use of the above two methods may lead to cold expansion and also result in better surface finish. There is no evidence in literature of the combined use of the above two methods.

2.2.6. Torsion and cold expansion method

Shamdani et al. [19] investigated numerical study using FEA software for the combined cold expansion and local torsion (CELT) on fastener holes. His study presumed that expansion is due to insertion of tapered tool and surface treatment is achieved by stirring action inside the hole. The schematic representation of local torsion is shown in fig.10.

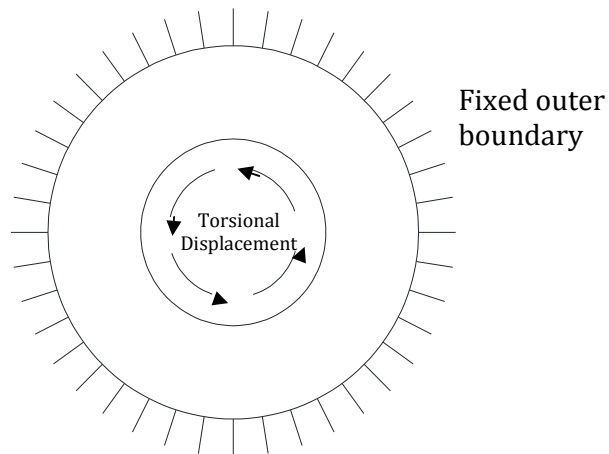


Figure 9 : Schematic representation of local torsion

The process of CELT and the induced residual stress distribution was studied. Maximum residual stresses which could be achieved as per the study was 100 percent of the maximum compressive stress of the material. It was observed that although local torsion as in the CELT process reduced the induced residual stresses as compared to cold expansion alone, strengthening was achieved by grain refinement. This would increase the overall mechanical performance of the hole.

2.2.7. Spherical mandrelling method

Maximov et al. [20] modeled a 3D finite element model of a spherical mandrelling process of cold expansion. The spherical mandrel performs a complex motion with respect to the stationary work piece which involves rotation about its own axis as well as the axis of the hole. This process can be done with conventional machines. The hole surface is improved by surface plastic deformation, better surface finish is achieved along with enhanced texture of the surface layer. The spherical mandrelling method is shown in fig. 9.

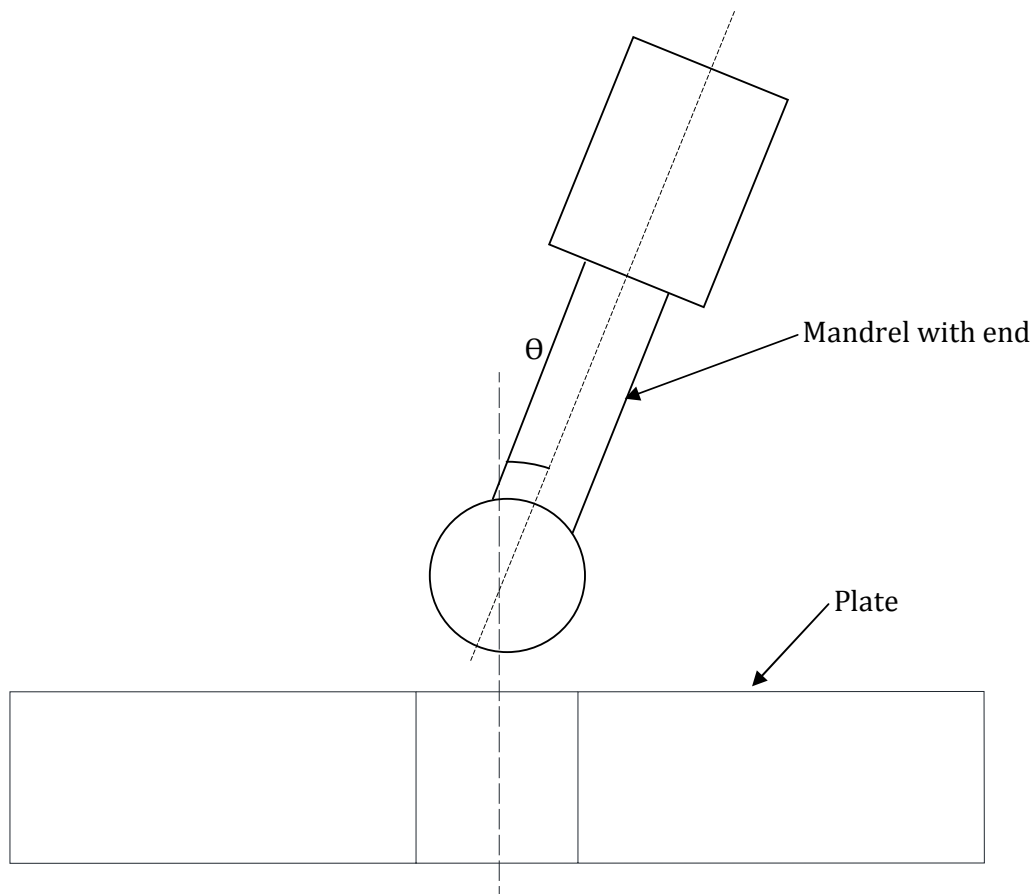


Figure 10 : Spherical mandrelling method

2.3. Gaps and Opportunity

Cold expansion operation done conventionally does not focus on the surface properties of the material. The surface roughness and hardness of the hole are important factors in determining the fatigue life of the component. Higher amount of surface roughness assist in the initiation of cracks and thereby leading to less fatigue life. Modification of the surface properties of the fastener holes to improve fatigue life have not been studied so far.

The conventional techniques of cold expansion have the following disadvantages :

- The conventional cold expansion technique has got heavy setup.
- Surface finish improvement may lead to better fatigue life. However, current cold expansion practices do not address it.
- Producing a composite layer has not been attempted.
- Also, the consideration of friction during cold expansion has not been studied.

Moreover, the cold expansion process has some practical limitations. There is possibility that the induced residual stresses may relax with time under repetitive straining and temperature variation. This problem can be solved by combining the cold expansion operation with surface treatment operations such as nanocomposite layering, carburizing, polishing and burnishing which will fill the interstices and other vacancies in the material and also increase surface hardness and fatigue life. These surface treatment operations lead to the formation of a finer grain structure. Severe plastic deformation (SPD) processing such as friction stir processing (FSP) can enhance mechanical properties of the material by grain refinement.

Advantages of Proposed Method

- A simple set-up can be used.
- Conventional CNC or milling machines can be used for cold expansion.
- The entire cold expansion process is completed in a single set-up.
- Saving of time and cost.

2.4. Problem Definition, Objective and Scope

2.4.1. Problem Definition

Fundamental study on rotation of tool during cold expansion and evaluation of effects on surface and mechanical properties thereby suggesting a variant of cold expansion method

2.4.2. Objective and Scope

The main objective of this study is to investigate the feasibility of cold expansion of a pre-drilled hole with a rotating tool and to assess the effect of the process on mechanical properties of the hole surface. The objective is also to study the effect of residual stress, surface roughness and hardness and their effect on fatigue life of the samples cold expanded using rotating tool and to assess the effect of burnishing on mechanical properties. An experimental study is proposed under different degrees of expansion 1.01%, 5.76%, 8.69%, using tapered tools of initial diameters of 9.2, 9.5, 9.9 mm and the maximum tool diameter is 10 mm. The induced residual stresses, hardness, surface finish and ovality of the holes are aimed to measure and relate with the fatigue life of cold expanded. Also, the fatigue life of cold expanded samples is compared with that of conventionally cold expanded samples. The material of the workpiece used in experiment is commercial aluminium and Al-2014-T6 aluminium alloy and the material of the tool is high speed steel. Three different tapered tools of diameters 9.2, 9.5 and 9.9 mm respectively are used resulting in 8.69, 5.26 and 1.01% degree of cold expansion. The maximum diameter of all the tools is 10mm. The feed rate of the tool during the cold expansion process is kept constant at 8mm/min and the rotation of the tool is 60 rpm.

Chapter 3

Material and Experimental Method

The present study is carried out on two different materials. A vertical milling machine is used for to carry out the RTCE experiments. The following section gives details about the process, materials and tools used and the experimental methods used for rotating tool cold expansion process.

3.1. Process Description

In the present study, cold expansion operation is carried out along with friction stirring of the hole surface, referred to as the rotating tool cold expansion (RTCE) process hereafter. A rectangular plate is used with a hole drilled at the centre of the plate. Three holes of different sizes, viz. 9.2 mm, 9.5 mm and 9.9 mm are cold expanded to a final diameter of 10 mm. An oversized tapered tool is used for this purpose. The diameter at the start of the taper is equal to the hole diameter while that at the end of the tapered portion is 10 mm. The tool is rotated with an rpm of 60 and a feed rate of 8 mm/min. The tool is inserted in the work piece till the entire tapered portion passes through the other end of the plate and then reverted back with the same speed and feed rate.

The tool insertion is done for an additional distance of 3 mm to ensure proper expansion of the entire hole surface. The edge of the tool at the bottom is chamfered to facilitate the initial entry of the tool. The RTCE is done for three different conditions: with metal working fluid (hereafter referred to as ‘wet condition’), without metal working fluid (hereafter referred to as ‘dry condition’) and dry with nano-sized particles (hereafter referred to as ‘nano condition’). Conventional water soluble coolant is used for this purpose.

The RTCE process may lead to a rough surface due to the material deformation caused by cold expansion and friction stirring combined. To improve the surface finish, the RTCE is followed by the burnishing operation. Two types of experiments are done: One involving RTCE and another one involving combined RTCE with burnishing. A roller burnishing tool

is used for the burnishing operation. The rotational speed used for burnishing is 2000 rpm and the feed rate is 1000 mm/min.

The drilling, RTCE and the burnishing operations are done consequently in the same set-up without altering the position of the work piece to avoid unsymmetrical axis and angular deviation during the process. The process is shown in fig. 3 and fig. 16. The process is carried out by different degrees of cold expansion. The amount of cold expansion being carried out is measured in terms of degree of cold expansion.

The degree of cold expansion (DCE) is defined by the relation :

$$DCE = \frac{(D-d)}{d} \times 100 \quad \dots (1)$$

where d is the diameter of the drilled hole and D is the diameter of the ball or tapered mandrel.

The conventional cold expansion performed for aerospace applications is in the range of 2% to 6% DCE. The specimens are drilled to diameters of 9.2 mm for 8.76 DCE, 9.5 mm for 5.26 DCE and 9.9 mm for 1.01 DCE respectively.

3.2. Material

Two different materials are used to study the process. For the first set of experiments, commercially available pure Aluminium is used while Al-2014-T6 Aluminium alloy is used for the second set of experiments. Aluminium sheet of 8 and 6 mm thickness and Al-2014-T6 Aluminium alloy sheet of 3 mm are used for the experiments. Work samples of 100 mm length are made from these sheets. The width of samples is 40 mm and 50 mm for Aluminium alloy and pure Aluminium respectively. The material property for the materials used is shown in Table 1. The chemical composition for the material used is shown in Table 2. Commercially available nano-sized alumina nano-sized particles (size<50 nm) is used.

Table 1 : Mechanical properties of material used

Material	Plate Thickness (mm)	Yield stress (MPa)	Ultimate tensile strength (Mpa)	Young's modulus E
Commercial Pure Aluminium	8 and 6	117.3	117.4	75.35
Aluminium Alloy Al- 2014 T6	3	470.17	488.17	70.23

Table : Chemical composition of material used

Material	Al	Cr	Cu	Fe	Mg	Mn	Si	Ti	Zn
Commercial Pure Aluminium	98.954	-	0.005	0.457	-	0.014	0.564	-	0.006
Al Alloy Al-2014 T6	91.66	0.03	3.969	0.302	2.337	0.758	0.861	0.028	0.065

3.3. Tools

The basic design of the tool has been depicted in Fig. 11. Three different tools are used for the cold expansion process. The initial diameters of the tools are 9.2 mm, 9.5 mm and 9.9 mm respectively while the final diameter is 10 mm. There is a tapered knurled portion for a length 15 mm until the final diameter is 10 mm which extends for the rest of the tool length.



Figure 11 : RTCE Tool

3.4. Machine and experimental set-up

The machine used for cold expansion is a vertical milling machine (VMM). Specimens of size 100 X 50 mm are cut using a wire-Electrical Discharge Machine (EDM). The work sample plate at the top is used as a dummy to aid in the cold expansion operation. A funnel shaped structure is fixed onto the top dummy plate to allow the Al_2O_3 nano-sized powder to enter the open space between the tool and the cavity during the cold expansion operation. The fixture arrangement is clamped over the dynamometer as shown in fig.12. The set-up used for experiments under nanoparticles, dry and wet cold expansion is as shown in fig. 12, fig.13, fig.14 and fig.15 respectively.



Figure 12 : Image of the set-up



Figure 13 : Image of the fixture for RTCE under nano condition

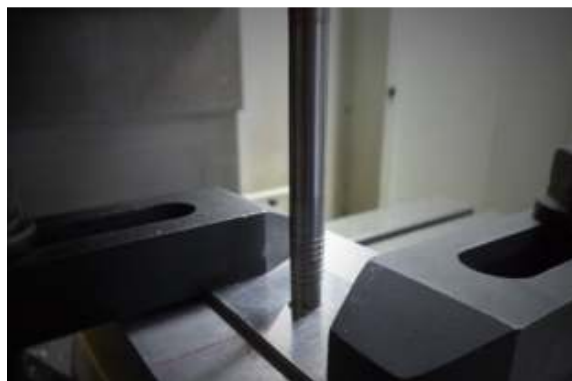


Figure 14 : Image of the fixture for RTCE under dry conditions



Figure 15 : Image of the fixture for RTCE under wet condition

3.5. Experimental Method

The RTCE is done in three different conditions : with metal working fluid (hereafter referred to as ‘wet condition’), without metal working fluid (hereafter referred to as ‘dry condition’) and dry with nano-sized particles (hereafter referred to as ‘nano condition’). Conventional water soluble coolant is used for this purpose. The specimens are firmly clamped on the fixture.

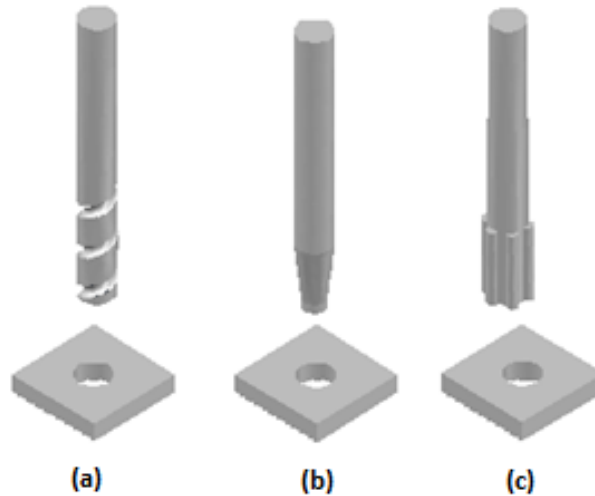


Figure 16 : Process flow – (a) Drilling, (b) Cold expansion, (c) Burnishing

The RTCE operation is performed on three different hole sizes : 9.2 mm, 9.5 mm and 9.9 mm. All these holes are expanded to the size of 10 mm. After the drilling operation, the over-sized rotating tool is inserted through the hole at a rotating speed of 60 rpm and a feed

of 8 mm/min and then retracted back with the same parameters. The cold expansion operation is followed by the burnishing process. The process flow is shown in fig. 16.

The same procedure is used for experiments performed under dry and wet conditions. While performing experiments under nano condition, a top plate and a funnel is used. The funnel is fitted in the slots formed in the top plate. The funnel is used to hold nano-sized particles and replenish it. Two types of experiments are done: One involving cold expansion and another one involving combined cold expansion with burnishing. A roller burnishing tool is used for the burnishing operation. The rotational speed used for burnishing is 2000 rpm and the feed rate is 1000 mm/min.

The burnishing operation has two major functions :

1. To smoothen the surface of the hole.
2. To enlarge the cold expanded specimens to a constant dimension to enable comparison of mechanical properties.

3.6. Measurement and Tests

3.6.1. Residual stress measurement

The X-Ray Diffraction machine is used to measure residual stresses of the cold expanded holes as shown in fig. . The X-ray diffraction is performed on a goniometer provided with detector. Radiation is used to collect data. The X-Ray measurements are performed at the entry and exit faces of the specimen. Each measured point corresponds to the center of one irradiated area. The measurement error of the machine is 20 MPa. The residual stress measurement set-up is shown in fig. 17.

3.6.2. Surface roughness and topography

The surface topography is measured using a Mahr Surface roughness testing machine (Marsurf XT 20). The topography is measured over an area of 1 mm X 1 mm on the central part of the cold expanded hole.

3.6.3. Ovality

The ovality of the cold expanded samples is measured using a Co-ordinate measuring machine. The diameter of the hole is measured at five positions of the hole at a depth of 1 mm, 2 mm, 3 mm, 4 mm and 5 mm respectively. Eight readings are taken to measure hole dimension. Three readings are taken at each position. Average of three readings is taken to enhance accuracy. The measurement positions are shown in fig. 18.

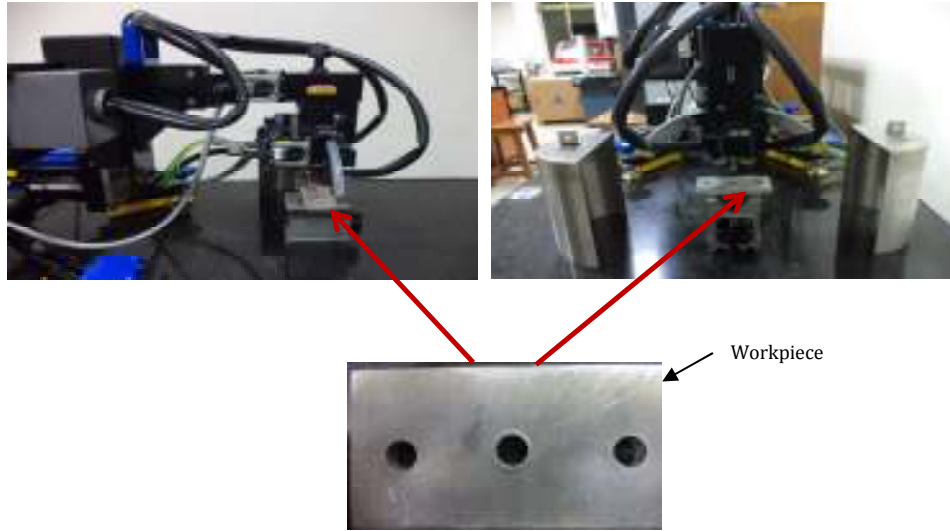


Figure 17 : Image of the X-Ray diffraction machine

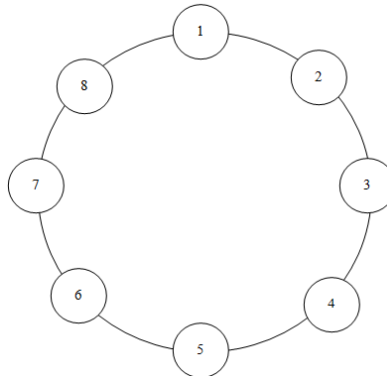


Figure 18 : Measurement positions for ovality showing periphery of the hole

3.6.4. Hardness distribution

The RTCE operated samples are cut vertically into two equal halves along the centre of the cavity to measure the hardness. This is done using wire-Electrical Discharge machine so that the hardness is minimally altered by the cutting process. The hardness of surface composite layers across the friction zone is measured using a Vickers hardness tester with a load of 100 kgf. Each hardness value is the average of three measurements.

3.6.5. Surface texture

SEM images are taken for the RTCE operated samples to compare the difference between the three RTCE mediums as well as to understand the effect of burnishing. SEM images are also taken for conventionally cold expanded samples for comparison with the RTCE process.

3.6.6. Fatigue life

Fatigue specimens of aluminium samples are produced as per ASTM E 466-07, as shown in fig. 19. The fatigue life assessment is carried out using a 100 kN capacity MTS UTM machine. The maximum stress value is kept at 105.6 MPa (nearly 0.9 times the yield strength) for fatigue test. The fatigue tests are carried out using constant amplitude, sinusoidal cyclic loads with a load ratio of $R = 0.1$ (P_{min}/P_{max}). A load frequency of 25 Hz is applied on the sample. The fatigue test specimen is as shown in figure 8. The 6 mm aluminium plates are milled to produce fatigue samples of 4 mm thickness. Aluminium alloy fatigue samples are made as per the same standard. The maximum stress value is kept at 211.6 MPa (nearly 0.45 times the yield strength) for fatigue test. The fatigue tests are carried out using constant amplitude, sinusoidal cyclic loads with a load ratio of $R = 0.1$ (P_{min}/P_{max}). A load frequency of 10 Hz is applied on the sample. The load vs. time graph is shown in fig. 20. The fatigue life testing arrangement is shown in fig. 21.

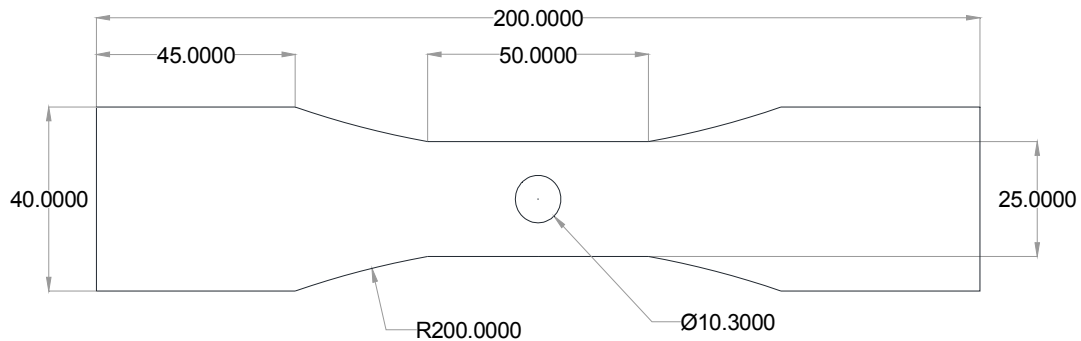


Figure 19 : Fatigue Test Sample

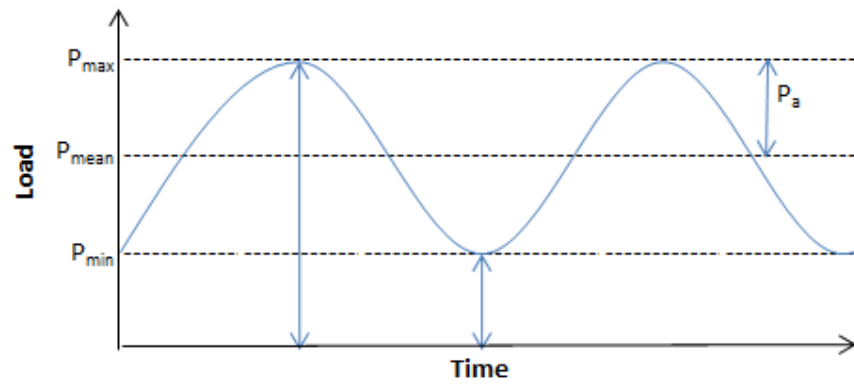


Figure 20 : Load vs. Time graph for constant amplitude sine load



Figure 21 : Fatigue Life Testing

Chapter 4

Results and Discussion

The results and discussions section is divided into two sub-sections for Al and Al-2014-T6 material. The results obtained for RTCE carried out using various mediums and at various degrees of cold expansion. The effects of parameters such as surface finish, residual stress and hardness on the fatigue life of rotating tool cold expanded (RTCE) holes is discussed. SEM images are taken to support the findings.

4.1. PART A : Pure Aluminium

4.1.1. Residual stresses

Friction between the tool and hole surfaces aids the RTCE process thereby achieving cold expansion at considerably low forces and also leads to induction of compressive residual stresses. The residual stresses induced are not high, possibly due to the sticking of the soft aluminium material during friction stirring. This effect may not be present if a relatively hard material is used for RTCE. In case of dry medium, RTCE at 8.76% DCE produces maximum residual stresses followed by that of wet medium and then by nano medium. The same is true for 1.01% DCE. The RTCE at 5.26 % DCE produces maximum residual stresses as compared to 1.01% and 8.76% DCE in case of nano medium. Moreover, RTCE at 5.26% DCE gives better results with nano particles as compared to dry and wet conditions. Cold expanded samples under nano conditions demonstrated more residual stresses as compared to those operated under dry and wet conditions. There is slight increase in the residual stresses due to the burnishing process. The graphs for maximum residual stress induced for various DCE's is shown in fig. 22. It seems that the combined cold expansion and burnishing process lead to pressing of hard nanoparticles on the surface of the hole. This increases the horizontal forces applied on the hole surface, which in turn results in higher residual stress in case of RTCE with nano medium. The residual stress distribution in the radial direction from the hole for 5.26% DCE shows a higher amount of residual stress followed by that of 8.76% and 1.01% DCE. This shows that a DCE of 5.26 is optimum. 1.01% DCE involves very less amount of cold expansion and hereby does not lead to any significant induction of residual stresses.

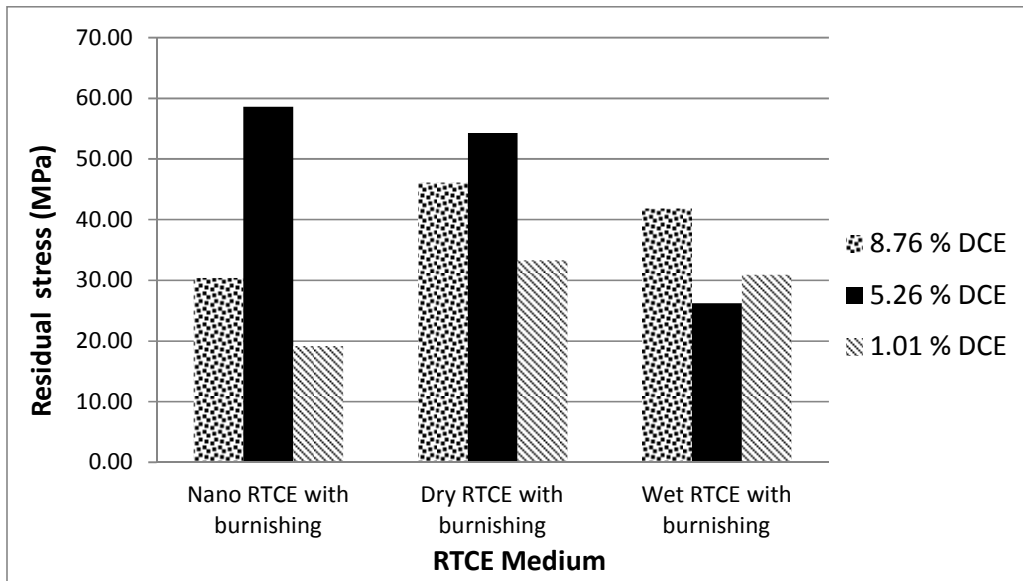


Figure 22 : Graph of residual stress for various DCE for RTCE

The critical DCE is known when the maximum equivalent Von Mises stress around the hole in the process of cold expansion reaches the ultimate tensile strength (yield strength for ductile materials). If the DCE exceeds the critical value, the maximum equivalent Von Mises stress will be greater than the ultimate tensile strength, and the fatigue life of such cold expanded holes will be lesser than the optimum fatigue life achievable. The graph for residual stress distribution for various degrees of cold expansion for nano condition is shown in fig. 23.

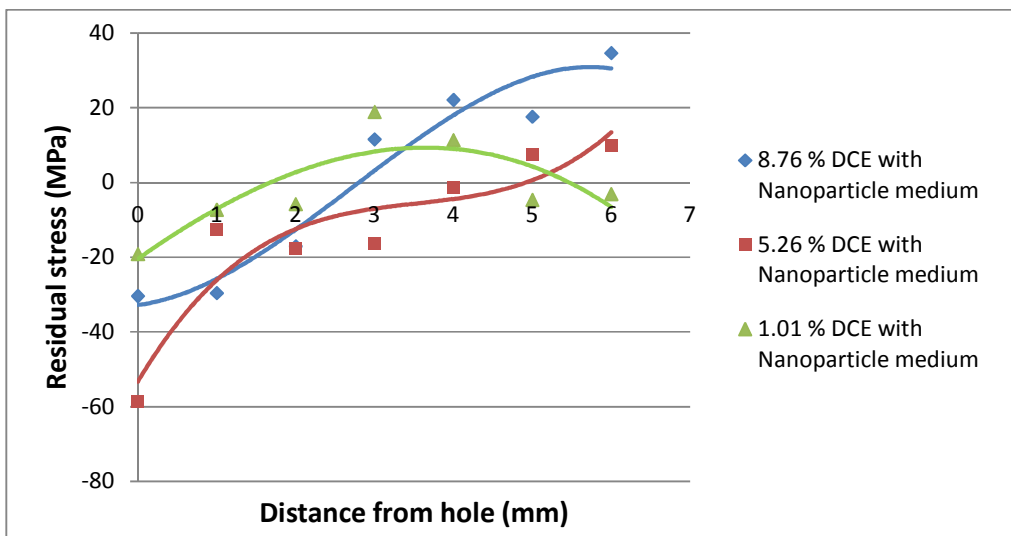


Figure 23: Graph of residual stress distribution for nano RTCE with burnishing for various DCE

The optimum degree of cold expansion can also be inferred from the force data for RTCE process. It can be seen that very high axial force is applied on the hole surface in case of RTCE with 8.76% DCE. Moreover, the maximum force is applied for a very small duration of time leading to impact and thereby damaging the hole surface which in turn results in lower residual stresses. Whereas in case of RTCE with 5.26% DCE, gradually increasing force is applied on the hole surface. The force vs. time graph is shown in fig. 24.

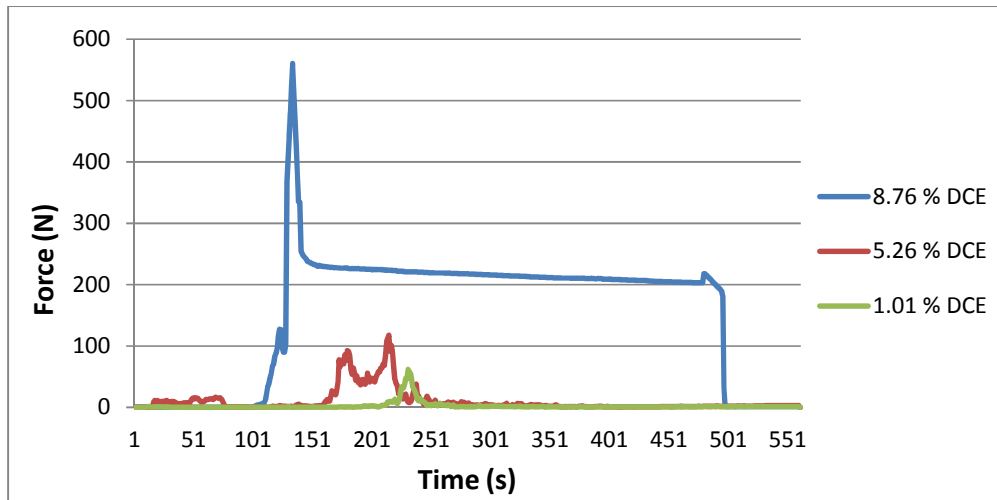


Figure 24 : Graph of axial force (F_z) vs. time for nano RTCE for various DCE

For frictional stirring to take place, sufficient amount of lateral forces should be applied on the surface of the hole during the RTCE operation to enable friction stirring and gradual deformation of the hole. At 5.26% DCE, maximum lateral force is applied as compared to 8.76% and 1.01% DCE which exhibit very less lateral force. The lateral force vs. time graph is shown in fig. 25.

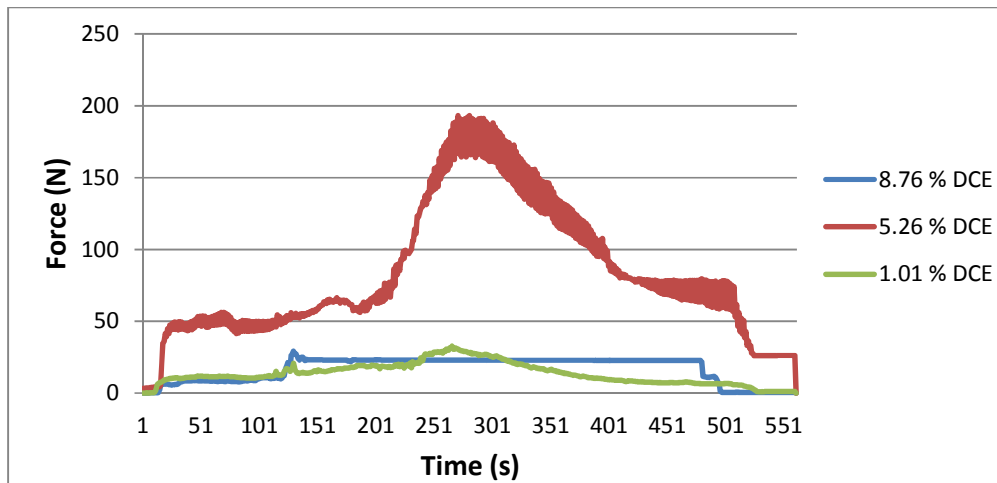


Figure 25 : Graph of lateral force (F_h) vs. time for nano RTCE for various DCE

The residual stress distribution in the radial direction from the hole for 5.26% DCE shows a higher amount of residual stress induced in case of RTCE under nano conditions followed by that of dry and wet condition. . The graph for residual stress distribution for RTCE at 5.26% DCE is shown in fig. 26.

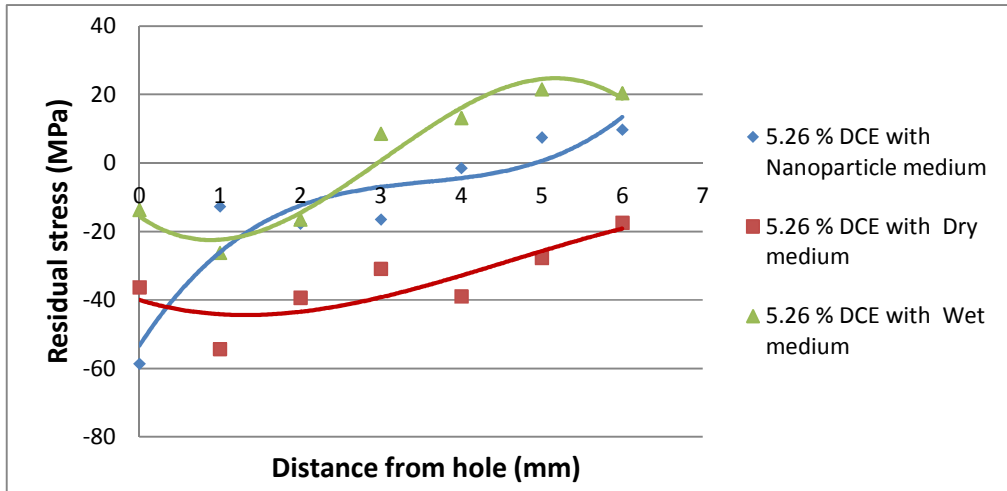


Figure 26 : Graph of residual stress distribution at 5.26 % DCE for nano RTCE with burnishing

Additional experiments are conducted on 6 mm Al plates having the same composition as that of 8 mm plates to study the impact of burnishing process on the residual stresses induced. Hardness and ovality are also measured using the same material. The graphs showing the residual stresses for burnished and unburnished samples are shown in fig. 27. The burnishing process leads to slight amount of cold expansion. It can be seen that the burnishing process results in significant improvement in residual stresses.

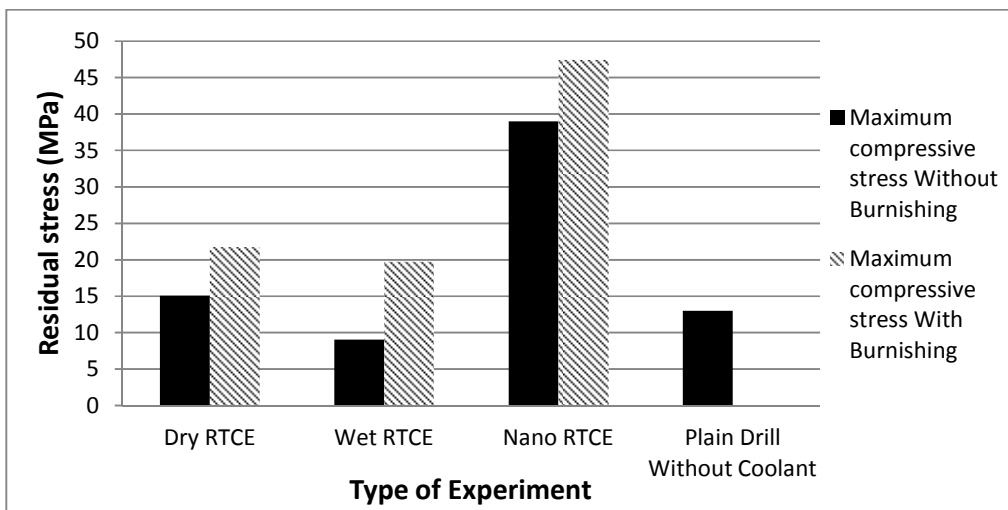


Figure 27 : Graph of residual stress for RTCE with and without burnishing for 5.26% DCE

4.1.2. Surface roughness

The magnitude of peaks and valleys is observed to be the least in case of wet RTCE samples followed by that of dry samples. The RTCE samples operated under nano condition showed more irregularities and higher amount of peaks and valleys. The surface roughness of the samples operated under dry and wet conditions is lower as compared to that of plain drilled samples. The nanoparticle operated samples has surface roughness nearly as that of the samples which are plain drilled without using coolant. After the burnishing process is employed, the surface roughness of the nanoparticle operated sample is reduced significantly to less than half the roughness of samples which are plain drilled without using coolant. The samples plain drilled with coolant have the least surface roughness. The surface roughness graphs showing Ra and Rz values are shown in fig. 28 and fig. 29 respectively. The burnishing process applies pressure on the peaks and the material gets filled in the valleys present on the hole surface during the stirring process. In the absence of peaks and valleys, even slightly higher amount of burnishing can lead to decrease in surface finish as in observed in case of RTCE with wet medium wherein the surface roughness has increased after the burnishing process.

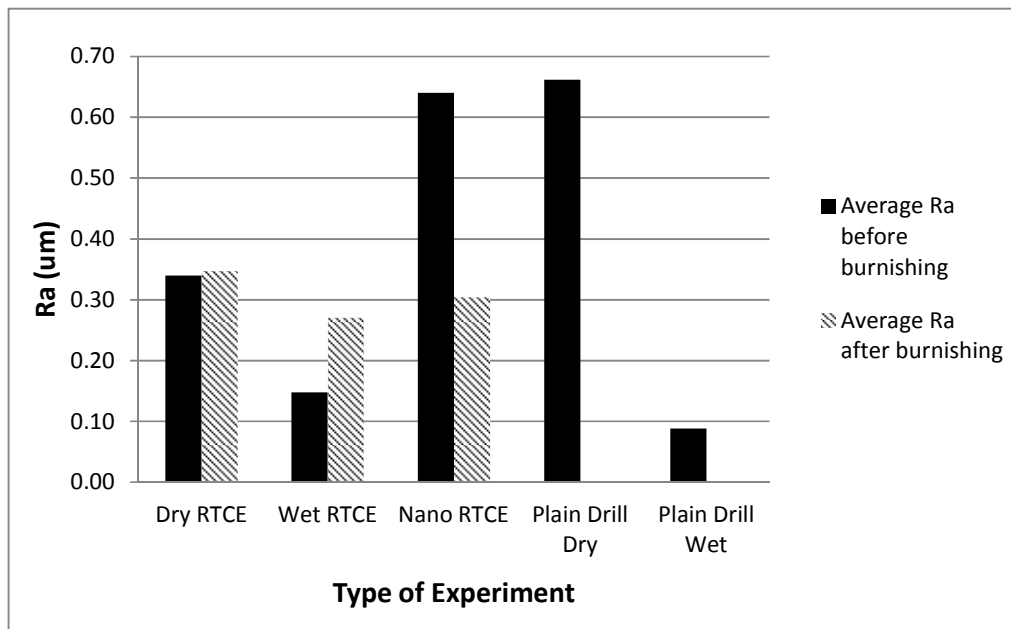


Figure 28 : Graph of surface roughness for Ra values for RTCE at 5.26% DCE

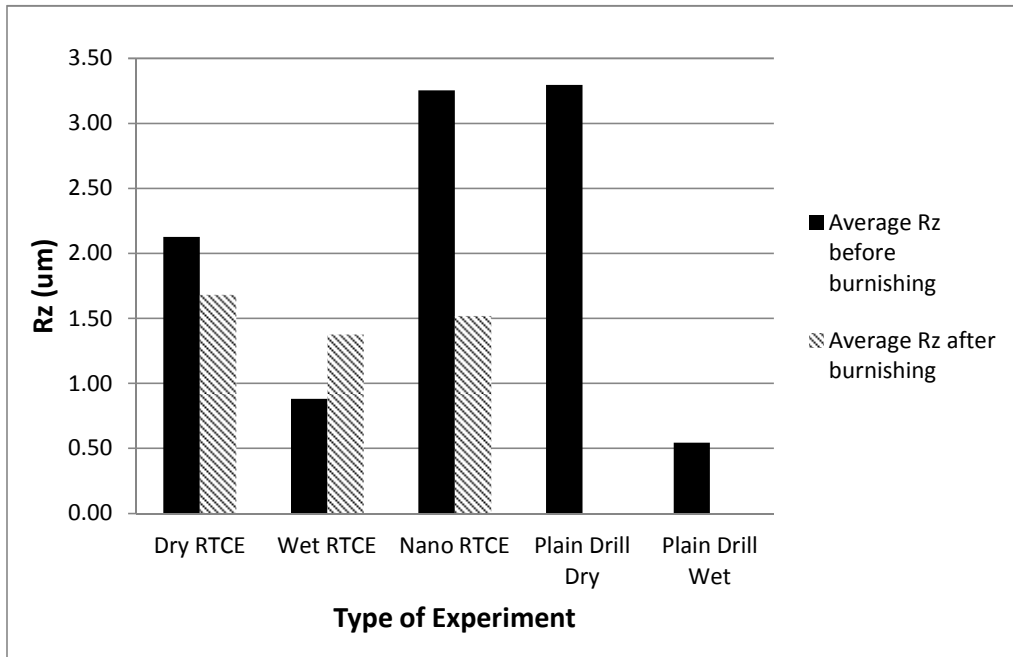


Figure 29 : Graph of surface roughness for Rz values for RTCE at 5.26% DCE

4.1.3. Surface topography

The magnitude of peaks and valleys is observed to be the least in case of wet RTCE samples followed by that of dry samples. The RTCE samples operated under nano condition showed more irregularities and higher amount of peaks and valleys. The surface topography results show that the magnitude of peaks and valleys is significantly reduced by the burnishing process. The rollers of the burnishing tool apply pressure on the hole surface and plastically deforms the projections. Some of the plasticized material also flows along the depth of the holes whereby the valleys get reduced to some extent due to material deposition caused by the pressure.

The surface topography has improved considerably in case of dry RTCE after the burnishing process. The magnitude of peaks and valleys has both reduced. Peaks and valleys of small magnitude, approximately one-third the size of the previous values exist as shown in fig. 30. and fig. 31. This finding can clearly be seen in the images shown in fig. 39(a) and fig. 39(b).

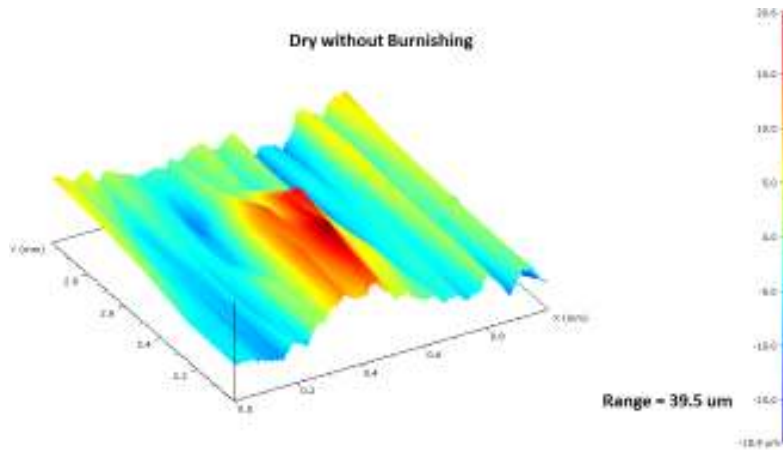


Figure 30 : Surface topography under Dry conditions for RTCE at 5.26 % DCE without burnishing

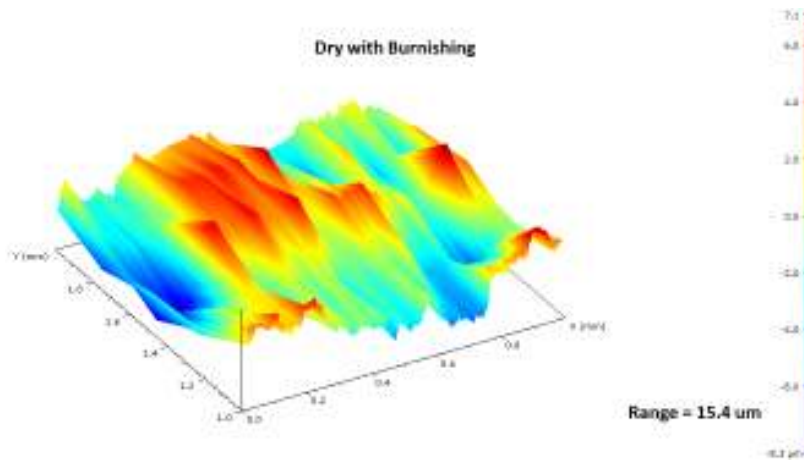


Figure 31 : Surface topography under Dry conditions for RTCE at 5.26 % DCE with burnishing

There are lots of serrations on the surface of the hole produced by wet RTCE. The magnitude of serrations has reduced by 20% and the magnitude of peaks and valleys decreased marginally. However the number of peaks and valleys has increased as shown in fig. 32. and fig. 33. This may be the result of over burnishing of the hole surface. Thus the surface roughness of the wet RTCE samples has increased as discussed in the previous section. This finding can clearly be seen in the images shown in fig. 39(c) and fig. 39(d).

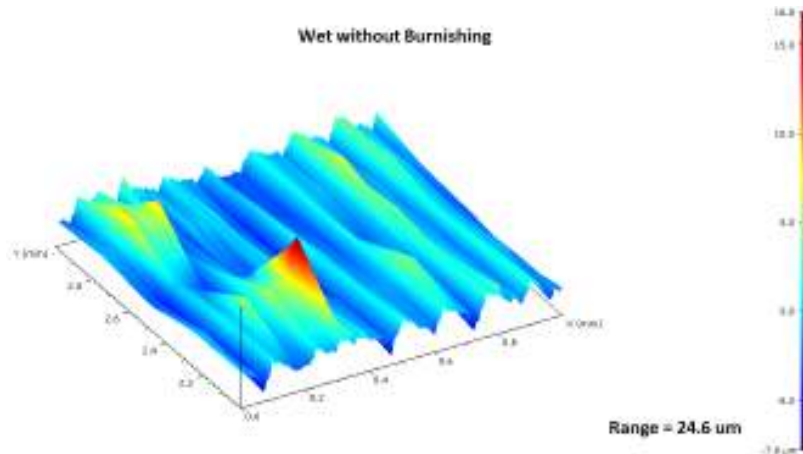


Figure 32 : Surface topography under Wet conditions for RTCE at 5.26 % DCE without burnishing

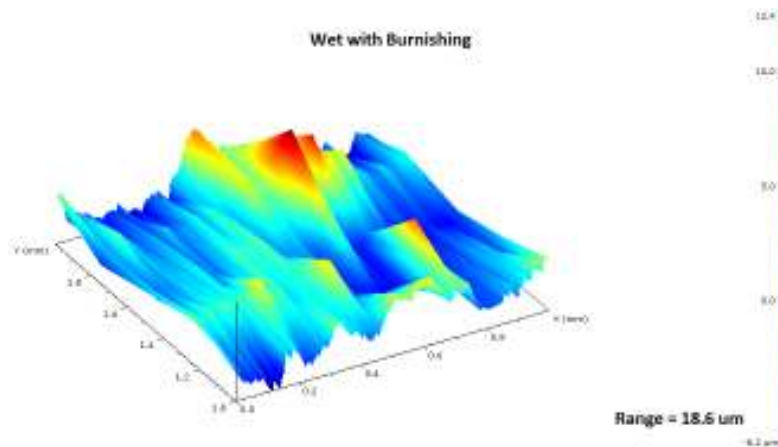


Figure 33 : Surface topography under Wet conditions for RTCE at 5.26 % DCE with burnishing

Serrations, peaks and valleys of large magnitude are found in case of nano RTCE. After the burnishing process, the serrations got removed. However, few peaks and valleys of half the value of the previous magnitude exist as shown in fig. 34. and fig. 35. Maximum improvement in surface topography was found in case of nano RTCE as compared to dry and wet RTCE. Thus the surface roughness of the nano RTCE samples has increased significantly as discussed in the previous section. This finding can clearly be seen in the images shown in fig. 39(e) and fig. 39(f).

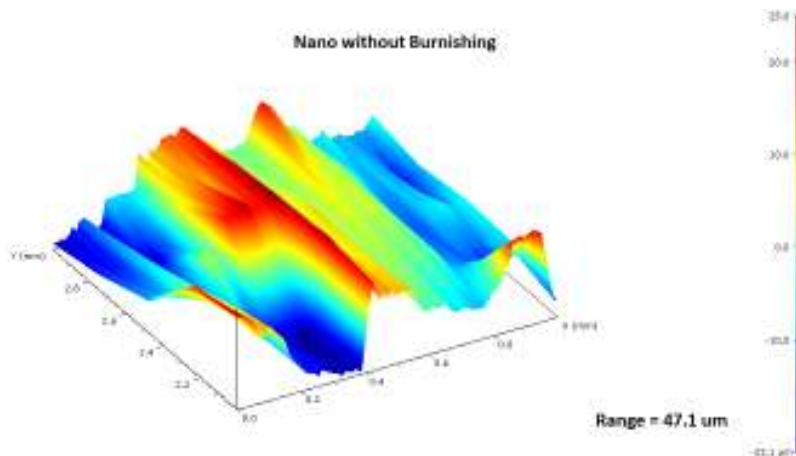


Figure 34 : Surface topography under Nano conditions for RTCE at 5.26 % DCE without burnishing

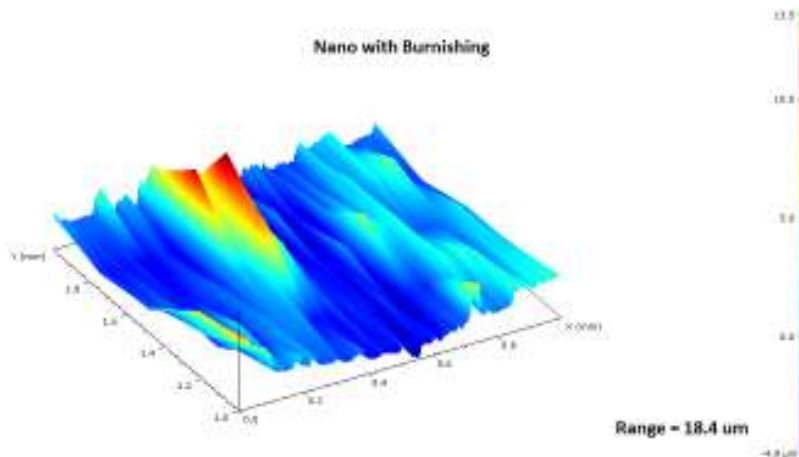


Figure 35 : Surface topography under Nano conditions for RTCE at 5.26 % DCE with and without burnishing

4.1.4. Ovality

The ovality for the holes with RTCE and RTCE with burnishing is measured. For the measured holes, the diameter of holes for wet condition is minimum at 10.06 mm followed by that of dry condition wherein the diameter is 10.15 mm. The diameter for nanoparticle condition is 10.26 mm. This implies that there is higher amount of spring back of the material in the elastic zone in case of wet and dry conditions. The cooling effect provided in the wet condition results in maximum contraction of the material immediately after RTCE. In case of nanoparticle condition, due to the higher pressure applied by the presence of nanoparticles combined with action of cold expansion process leads to more amount of cold expansion, thereby resulting in a hole of larger diameter. The ovality is shown in fig. 36.

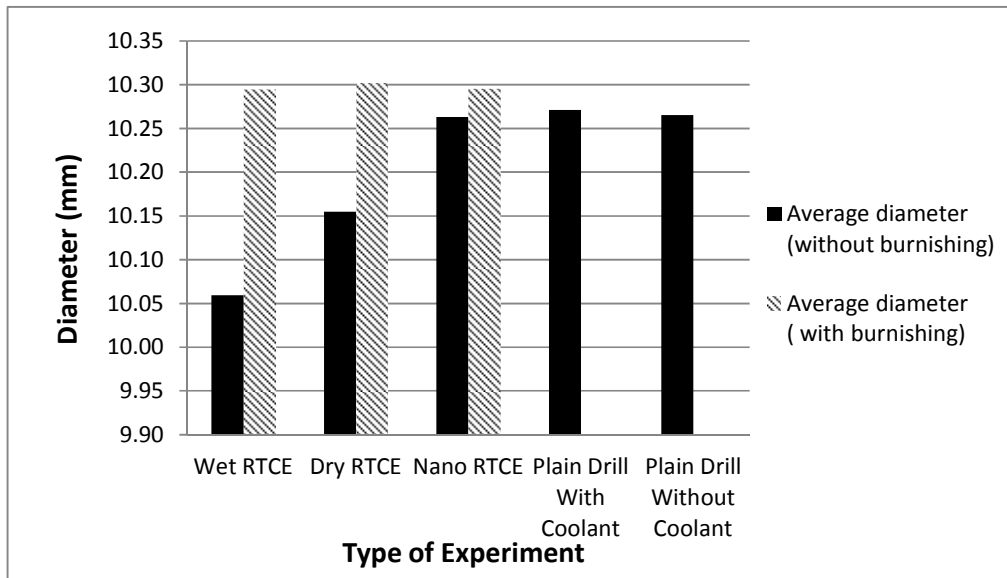


Figure 36 : Ovality measurement for RTCE at 5.26% DCE

4.1.5. Hardness

The hardness value of samples with hole drilled without coolant and with coolant is 67.91 and 65.345 HRB respectively. The combined cold expansion with burnishing processes resulted in an increase in hardness. The increase in hardness over the samples drilled with coolant is found to be highest, about 37.7 %, in case of RTCE with nanoparticles. This increase in hardness is mainly due to the embedding of nanoparticles over the hole surface. Slight amount of grain refinement also occurs due to the tool stirring action. There is approximately 12.8 % increase in hardness in case of RTCE under dry conditions. There is no significant increase of hardness in RTCE under wet condition. The reason for this could be the loss of hardness due to the elastic spring back of the material around the vicinity of

the hole after the RTCE operation. The hardness measured for RTCE and plain drilled samples is shown in fig. 37.

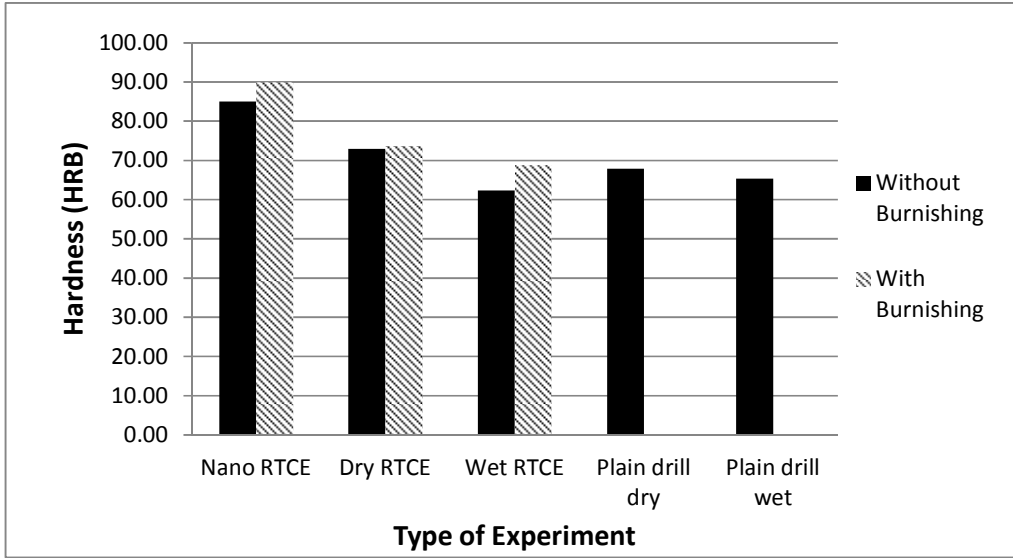


Figure 37 : Hardness measurement for RTCE at 5.26% DCE

4.1.6. Surface texture

The RTCE process causes stirring of the material on the surface of the hole. This can be seen by the flow lines created on the surface is shown by the SEM images in fig. 39, fig. 39(a), fig. 39(c) and fig. 39(e) respectively. The pattern of flow appears to be much more prominent after the burnishing process. The burnishing process also reduces the surface irregularities. This effect is demonstrated in fig. 39(b), fig. 39(d) and fig. 39(f) respectively. Higher amount of surface material plastic deformation is observed in case of nano medium due to the stirring action and additional pressure caused by the presence of nanoparticles. Negligible change in surface is observed in case of conventional cold expansion (CCE) as shown in fig. 38.

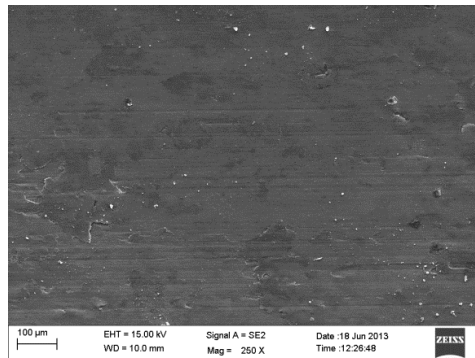


Figure 38 : SEM image showing texture of cylindrical wall for CCE at 5.26 % DCE

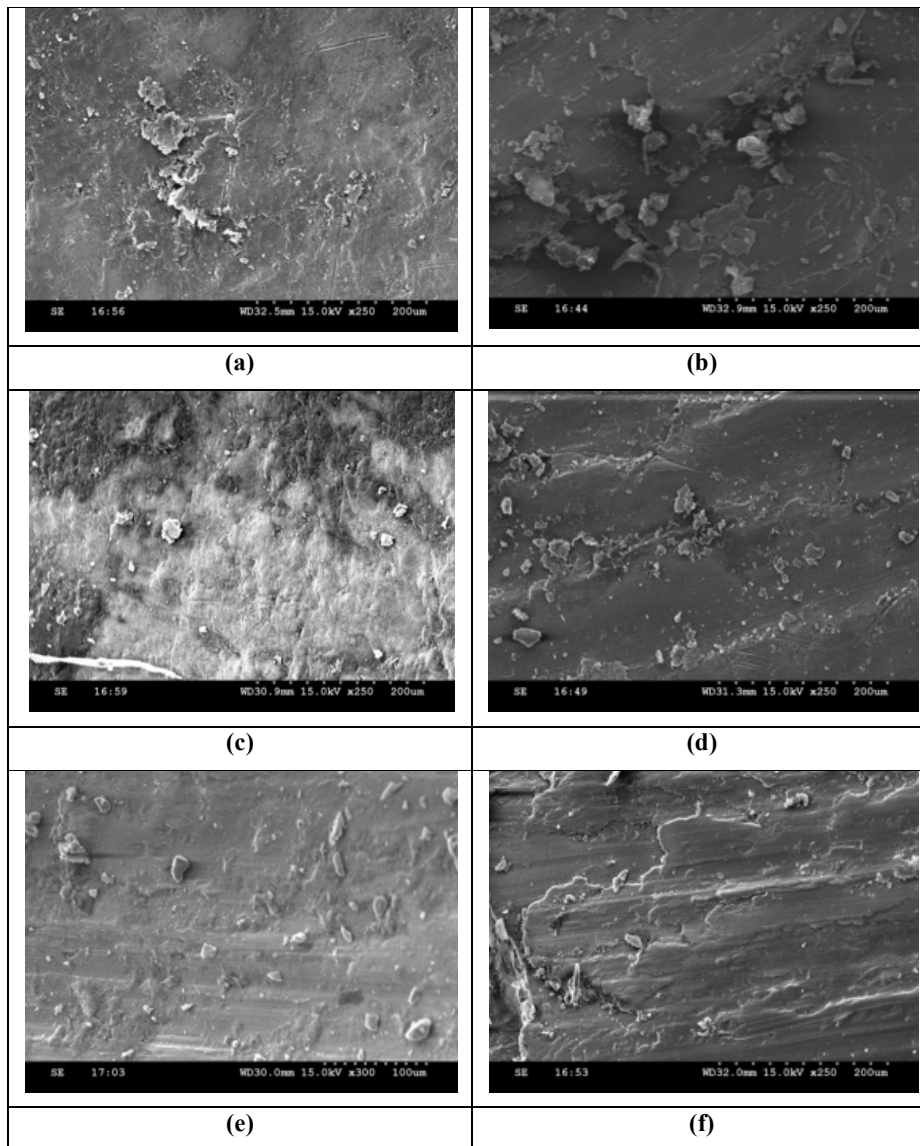


Figure 39 : SEM images showing texture of cylindrical wall for various conditions of (a) Wet RTCE without Burnishing, (b) Wet RTCE With Burnishing, (c) Dry RTCE without Burnishing, (d) Dry RTCE With Burnishing, (e) Nano RTCE without Burnishing, (f) Nano RTCE With Burnishing for Aluminium material at 5.26% DCE.

4.1.7. Fatigue life

The number of cycles to failure of the RTCE operated specimens without burnishing of the holes and with hole burnishing are presented in Table 3. The fatigue life of RTCE samples is improved after the burnishing process, as shown in fig. 40. Fatigue life is higher for unburnished nano and wet samples as compared to plain drilled sample. Unburnished dry sample life is lower than that of plain drilled sample due to more surface roughness. Maximum amount of burnishing is done for wet sample followed by dry sample. Therefore the improvement in fatigue life for wet sample after burnishing is the highest. Least amount of burnishing is done for nano sample. So the improvement in fatigue life after burnishing is lesser in case of nano. Maximum fatigue life is observed in case of nano samples. This may be due to the improvement in the surface finish, hardness and induction of compressive residual stresses due to additional pressure created due the presence of nanoparticles.

Table 3 : Fatigue life of RTCE operated specimens

RTCE Medium	Fatigue Life Without Burnishing	Fatigue Life With Burnishing
Dry RTCE	9499	19144
Wet RTCE	18456	32685
Nano RTCE	29342	34182
Plain Drill	16518	-

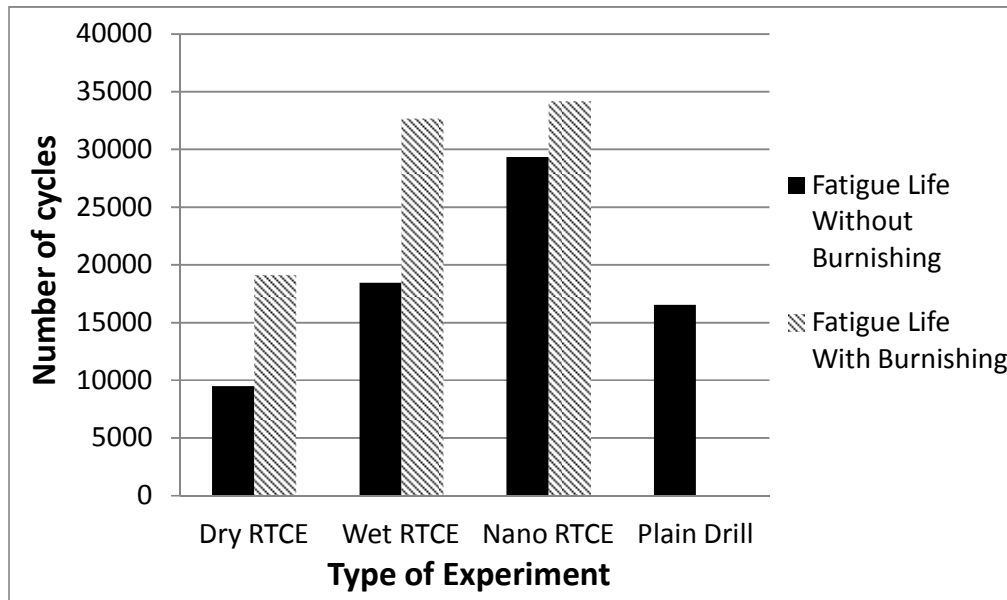


Figure 40 : Fatigue Life for RTCE at 5.26% DCE

4.1.7.1. Effect of residual stress on fatigue life

The nanoparticles fill up the cracks on the surface of the hole and also makeup for the material loss. This effect is known as mending effect. Kwangho Lee et. al also observed this effect during their study on role of nanoparticles in lubrication [21]. During fatigue cycles, the cracks open up during tensile loading. However, during the compression cycle, the nanoparticles arrest the closing of cracks. The loads are applied in the tensile mode only, thereby leading to more fatigue life.

The fatigue life of RTCE specimens is compared with the induced residual stress as shown in fig. 41. It can be observed that the fatigue life is proportional to residual stress. RTCE under wet condition shows proportionately higher fatigue life. This can be attributed to the higher surface finish achieved in case of wet samples as compared to that achieved in case of RTCE under nano and dry conditions.

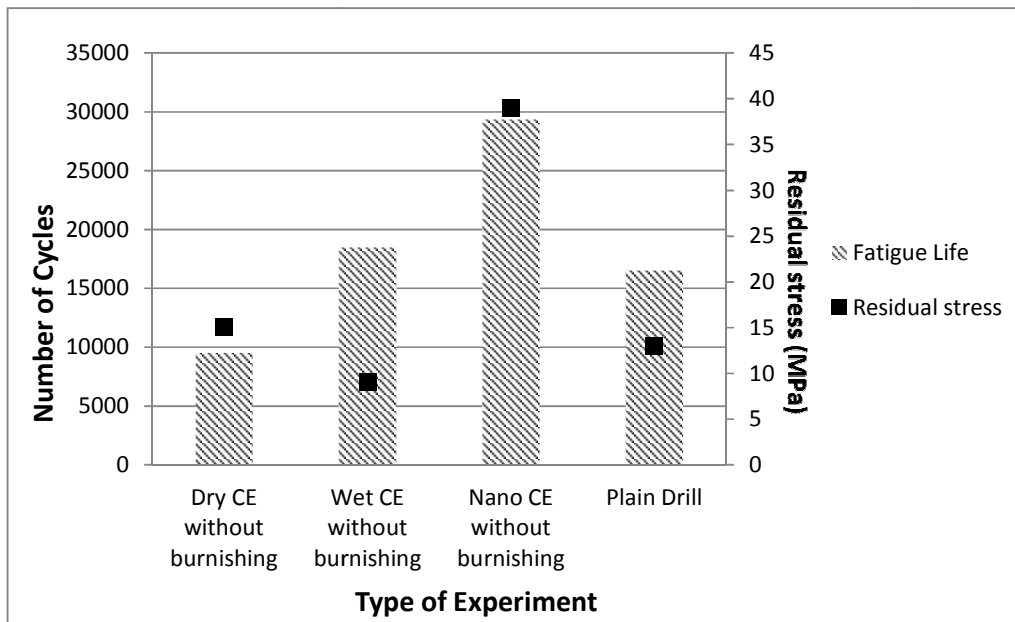


Figure 41 : Comparison of Fatigue life with Residual stress for RTCE at 5.26% DCE and CCE specimens

Conventional cold expansion (CCE) process is also carried out using a tapered tool for three degrees of cold expansion : 8.76% DCE, 5.26% DCE and 1.01% DCE. This process is carried out on a 100 kN capacity UTM machine (MTS make).The set-up for CCE is shown

in fig. 42. The initial diameters of the tool to achieve 8.76%, 5.26% and 1.01% DCE are 9.2 mm, 9.5 mm and 9.9 mm. The tool is shown in fig. 43.

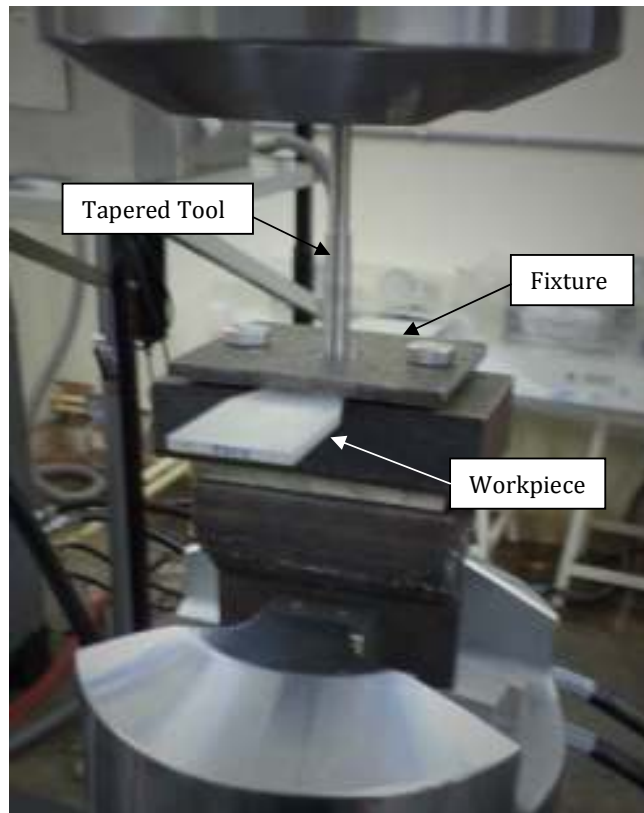


Figure 42 : Conventional cold expansion set-up



Figure 43 : Tapered tool used for conventional cold expansion

Fatigue testing is carried out for the conventionally cold expanded samples. The comparison of fatigue life with residual stress for RTCE and CCE specimens is shown in fig. 44. The fatigue life for CCE is proportional to residual stress induced. CCE with 5.26% DCE shows

the highest fatigue life as compared to that achieved with 8.69% and 1.01% DCE. Therefore 5.26% is the optimum DCE for 10 mm basic hole size. It is also observed that the CCE at 8.76% DCE results in lower fatigue life as compared to the residual stresses induced. This can be the results of sub-surface cracks due to extreme cold expansion.

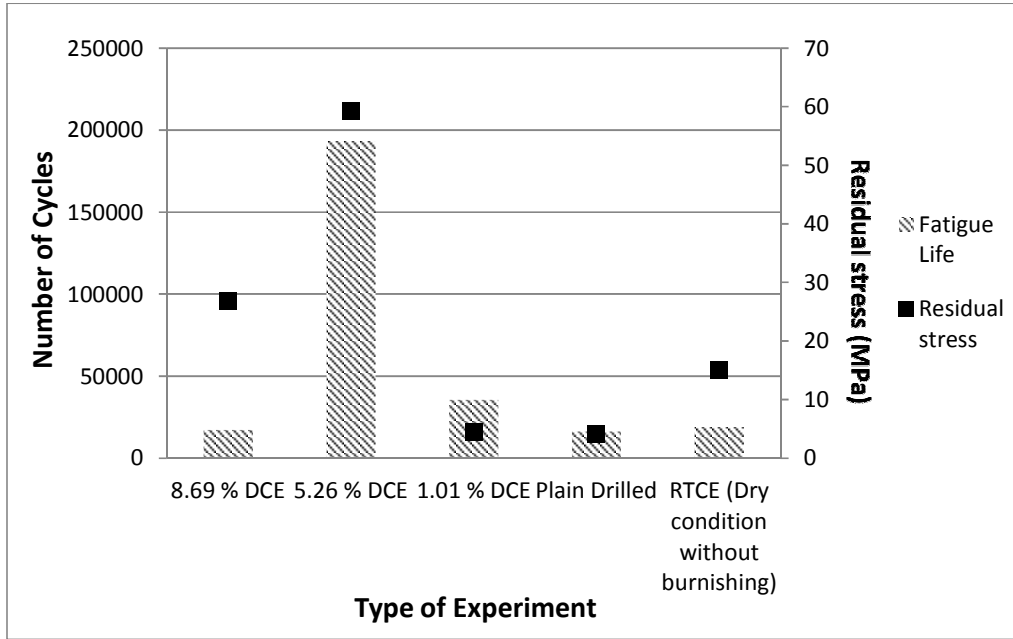


Figure 44 : Fatigue life and Residual stress comparison for RTCE at 5.26% DCE and CCE

4.1.7.2. Effect of surface roughness on fatigue life

Surface roughness is an important factor that can affect crack initiation on the hole surface and thereby lead to fatigue failure. The comparison of fatigue life with surface roughness is shown in fig.45 to fig. 48. In case of dry RTCE, although the Ra values are not affected much after the burnishing process, there is a considerable drop in Rz values and the fatigue life has increased by a little more than 100%. In case of wet RTCE, although the Ra value has increased marginally post burnishing, there is significant drop in Rz value. We can also see approximately 77% improvement in fatigue life. In case of nano RTCE, although very small amount of burnishing is possible because of the already increased hole size, there is a fair improvement of fatigue life after burnishing. The Ra and Rz values have both reduced post burnishing operation for nano RTCE. These results that surface roughness is inversely proportional to fatigue life.

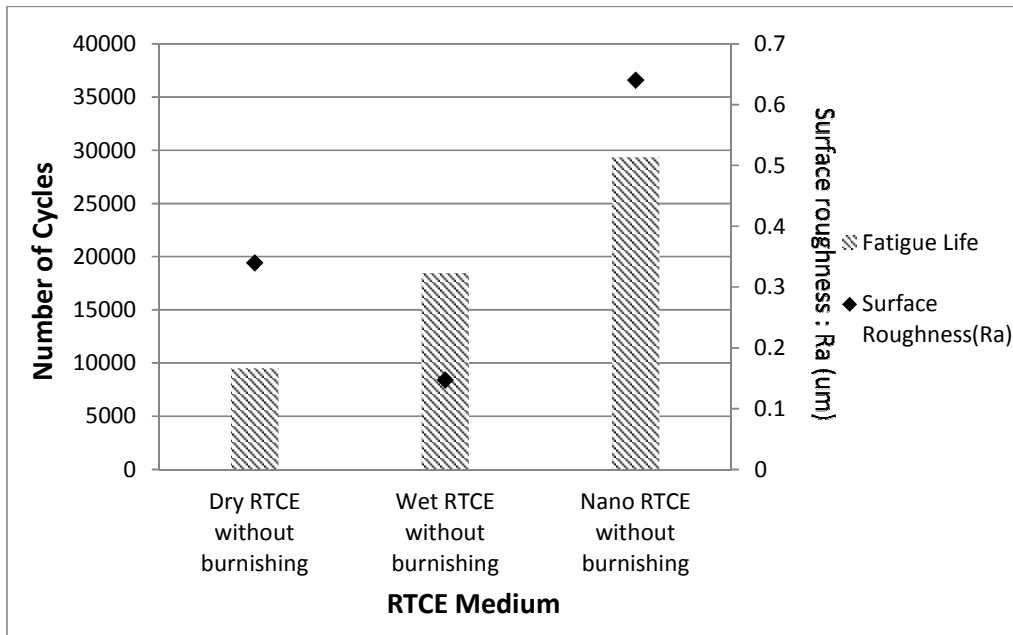


Figure 45 : Fatigue life and Surface roughness (Ra) comparison for RTCE at 5.26% DCE without burnishing

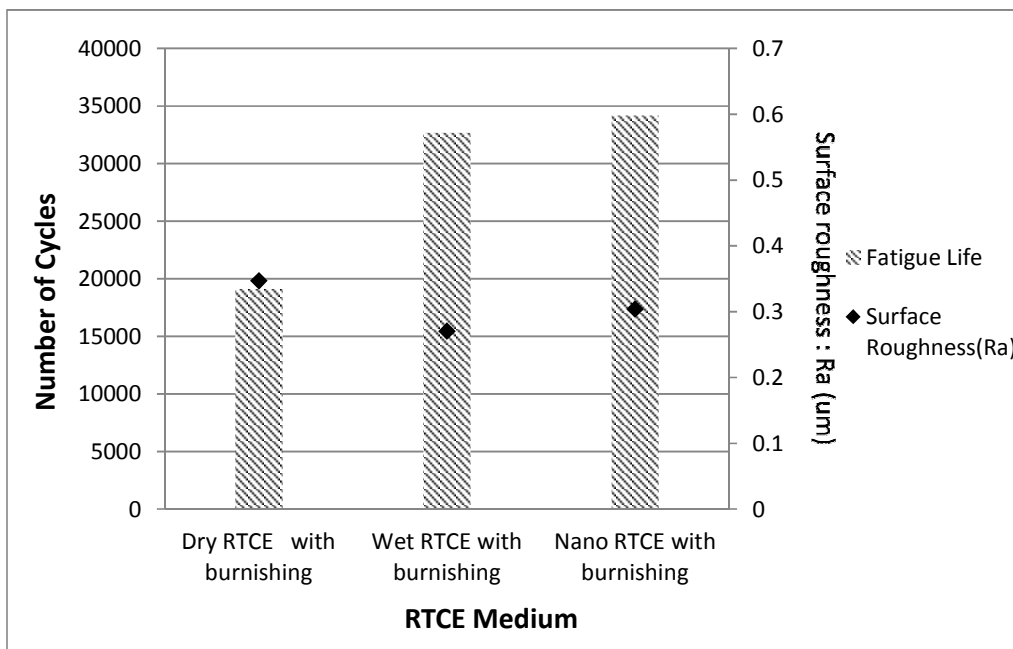


Figure 46 : Fatigue life and Surface roughness (Ra) comparison for RTCE at 5.26% DCE with burnishing

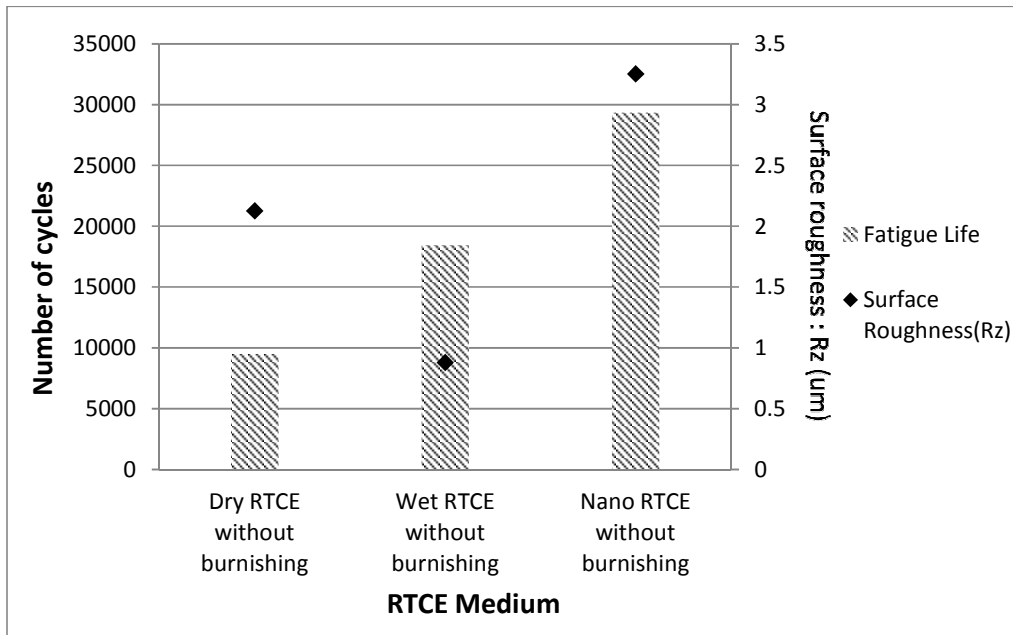


Figure 47 : Fatigue life and Surface roughness (Rz) comparison for RTCE at 5.26% DCE without burnishing

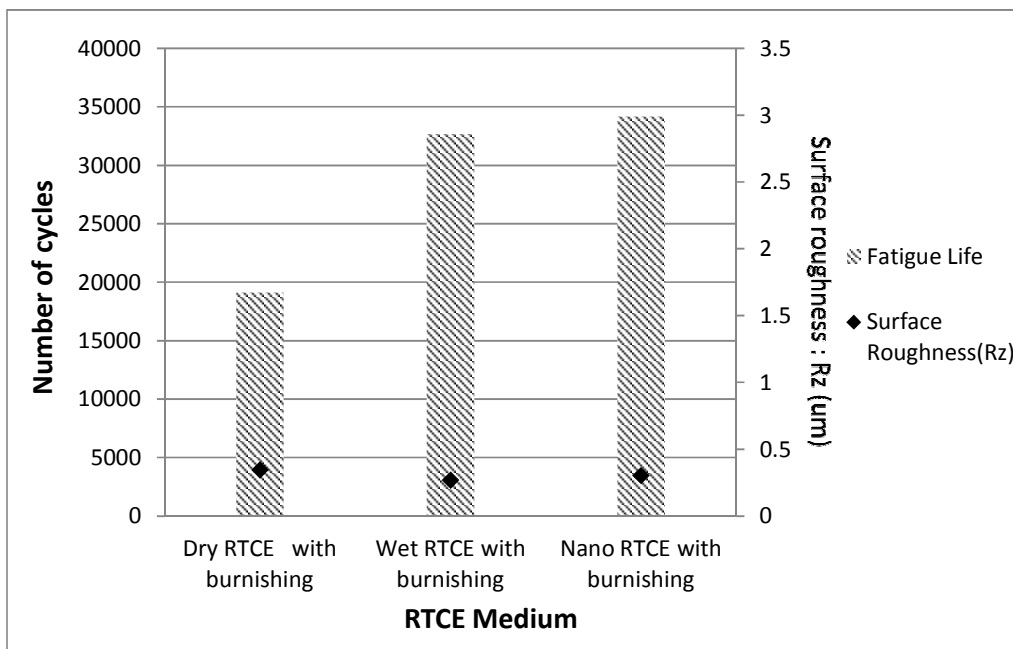


Figure 48 : Fatigue life and Surface roughness (Rz) comparison for RTCE at 5.26% DCE with burnishing

4.1.7.3. Effect of hardness on fatigue life

The comparison of fatigue life vs. hardness is shown in fig. 49 and fig. 50. It can be observed that in case of dry and nano RTCE, there is no significant improvement in hardness after burnishing but there is marginal improvement in fatigue life for nano RTCE and approximately 200% improvement of fatigue life for dry RTCE. The improvement in fatigue life for dry RTCE is due to the better surface finish achieved and the residual stresses induced. In case of wet RTCE, there is approximately 10% improvement in hardness. The fatigue life for wet RTCE has increased by approximately 77% post burnishing. However, this improvement in fatigue life is more likely because of the better surface finish and the residual stress induced. These findings are not sufficient to explain the exact effect of hardness on fatigue life. The relationship of hardness with fatigue life can be seen more prominently in case of RTCE with Al-2014 T6 alloy which will be discussed later.

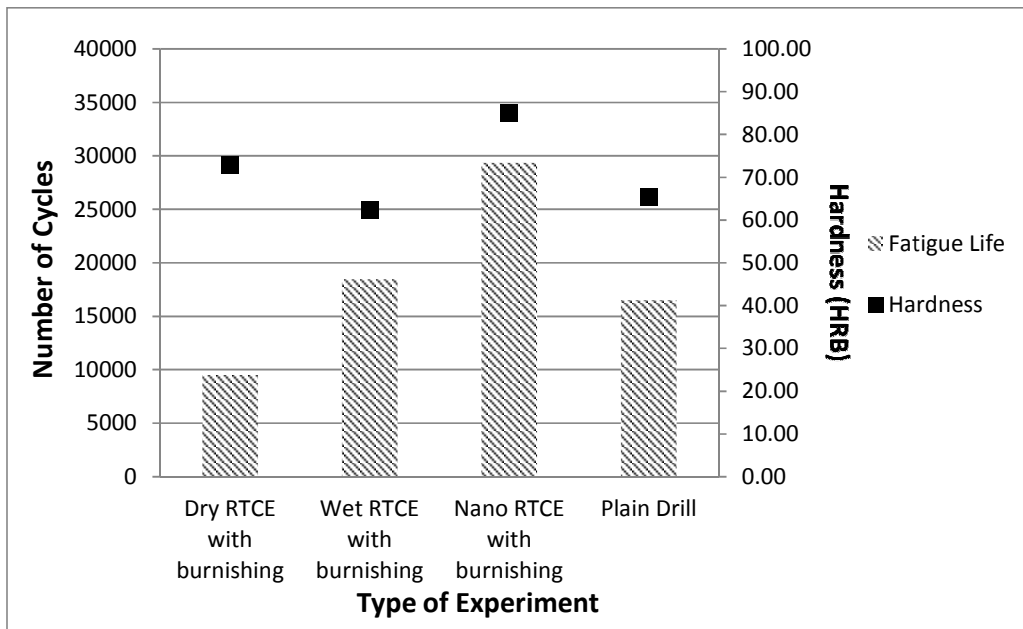


Figure 49 : Fatigue life and Hardness comparison for RTCE without burnishing at 5.26% DCE

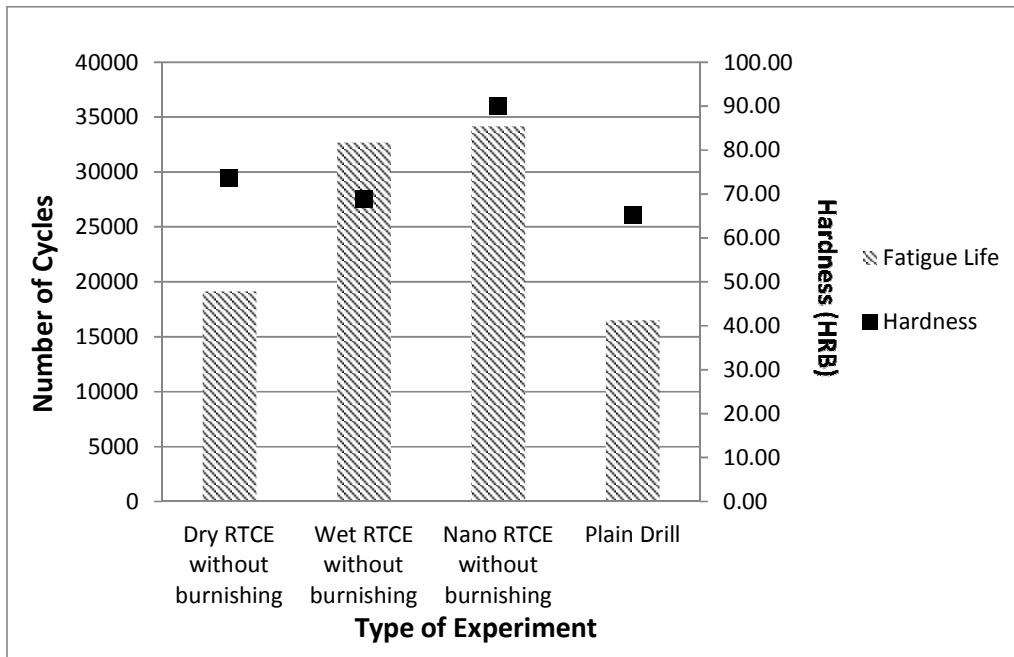


Figure 50 : Fatigue life and Hardness comparison for RTCE with burnishing at 5.26% DCE

4.2. PART B : Aluminium Alloy- Al 2014-T6

4.2.1. Residual stresses

Friction between the tool and hole surfaces aids the RTCE process thereby achieving cold expansion at considerably low forces and also leads to induction of compressive residual stresses. The residual stresses induced in dry and wet conditions are approximately the same. Slightly lower residual stresses are induced in the sample operated under nano conditions. There is downward flow of surface material in case of dry and wet operated samples. This effect is not found in the nano operated samples. It seems that the nanoparticles act as a lubricant during the cold expansion process. After the burnishing process, the nano operated samples have maximum residual stresses followed by wet and then by dry samples. The higher amount of residual stresses induced while burnishing in the nano operated samples may be due to the higher pressure applied by the nanoparticles on the hole surface. In all the conditions, significant amount of improvement in residual stresses is observed as compared with that of plain drilled sample. The residual stresses induced in the RTCE samples and the effect of burnishing is shown in fig. 51.

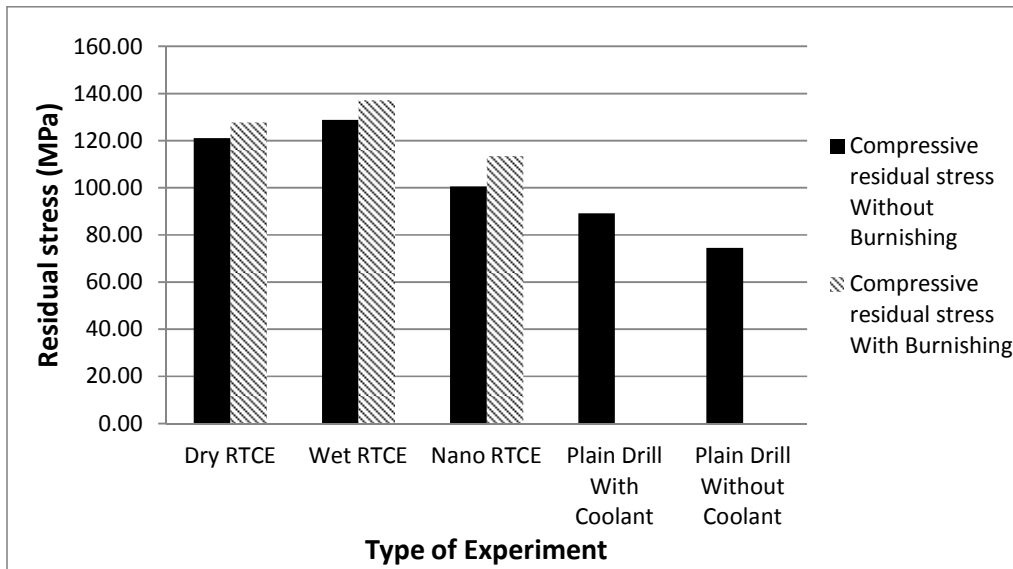


Figure 51 : Graph of residual stress for RTCE at 5.26% DCE for three conditions with and without burnishing

4.2.2. Surface roughness

The magnitude of peaks and valleys is observed to be the least in case of wet RTCE samples followed by that of dry samples. The RTCE samples operated under nano condition showed more irregularities and higher amount of peaks and valleys. The surface roughness of the samples operated under dry and wet conditions is lower as compared to that of plain drilled samples. The nanoparticle operated samples have surface roughness nearly as that of the samples which are plain drilled without using coolant. After the burnishing process is employed, the surface roughness of the nanoparticle operated sample is reduced significantly to less than half the roughness of samples which are plain drilled without using coolant. The samples plain drilled with coolant have the least surface roughness. The surface roughness graphs showing Ra and Rz values are shown in fig. 52 and fig. 53 respectively.

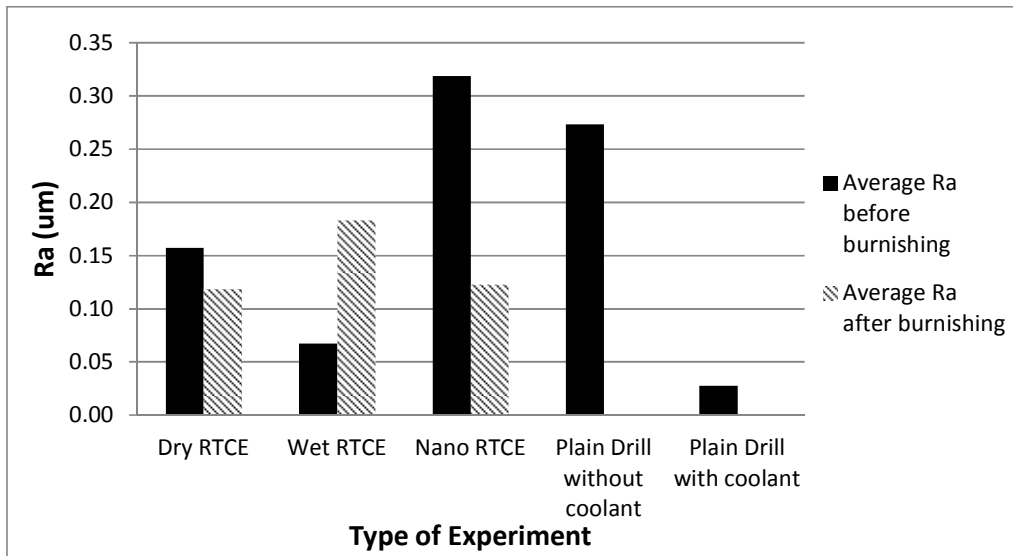


Figure 52 : Graph of surface roughness for Ra values for RTCE at 5.26% DCE

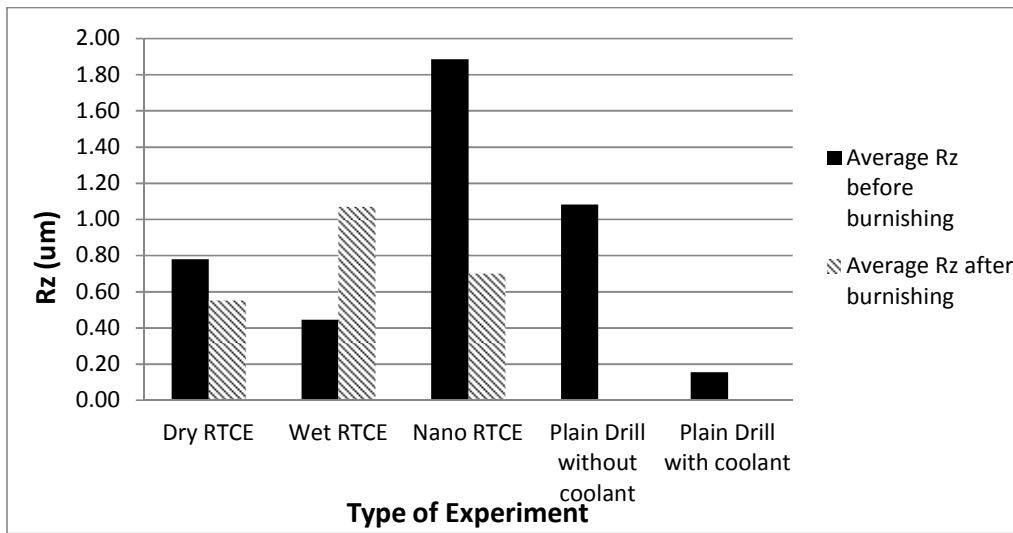


Figure 53 : Graph of surface roughness for Rz values for RTCE at 5.26% DCE

4.2.3. Surface topography

The surface topography results show that the magnitude of peaks and valleys is significantly reduced by the burnishing process. The rollers of the burnishing tool apply pressure on the hole surface and plastically deforms the projections. Some of the plasticized material also flows along the depth of the holes whereby the valleys get reduced to some extent due to material deposition caused by the pressure. The surface topography has improved considerably in case of dry RTCE after the burnishing process. The magnitude of peaks and

valleys has both reduced. Peaks and valleys of small magnitude, approximately one-fourth the size of the previous values exist as shown in fig. 54. and fig. 55. This finding can clearly be seen in the images shown in fig. 62(a) and fig. 62(b).

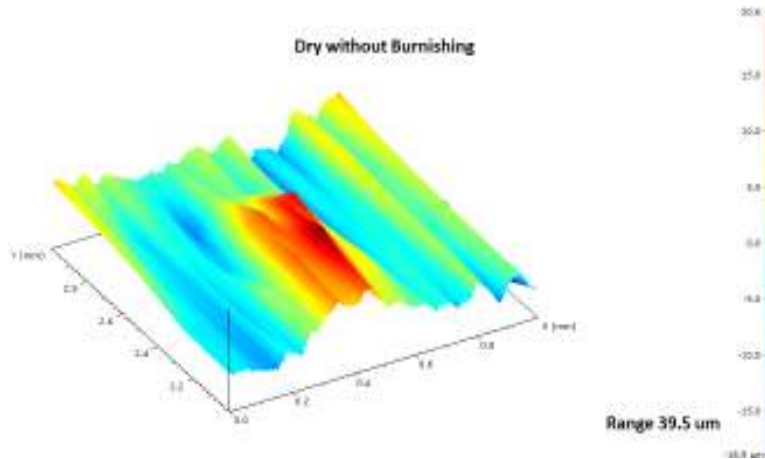


Figure 54 : Surface topography under Dry conditions for RTCE at 5.26 % DCE without burnishing

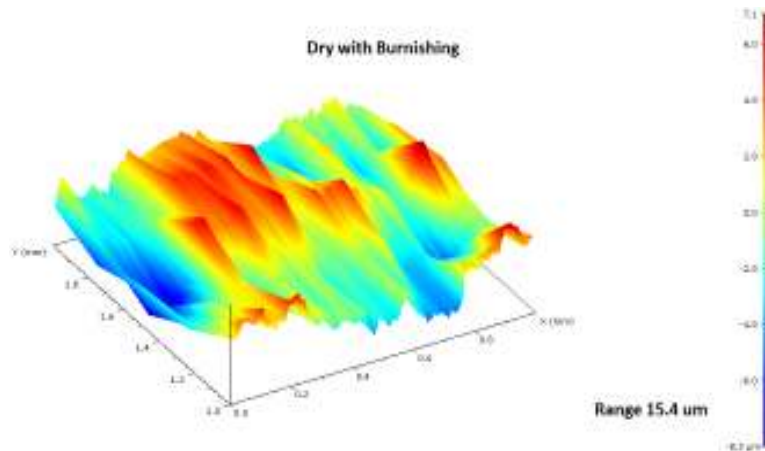


Figure 55 : Surface topography under Dry conditions for RTCE at 5.26 % DCE with burnishing

There are lots of serrations on the surface of the hole produced by wet RTCE. The magnitude of serrations has reduced by 20% and the magnitude of peaks and valleys decreased marginally. However the number of peaks and valleys has increased as shown in fig. 54. and fig. 55. This may be the result of over burnishing of the hole surface. Thus the surface roughness of the wet RTCE samples has increased as discussed in the previous section. This finding can clearly be seen in the images shown in fig. 62(c) and fig. 62(d).

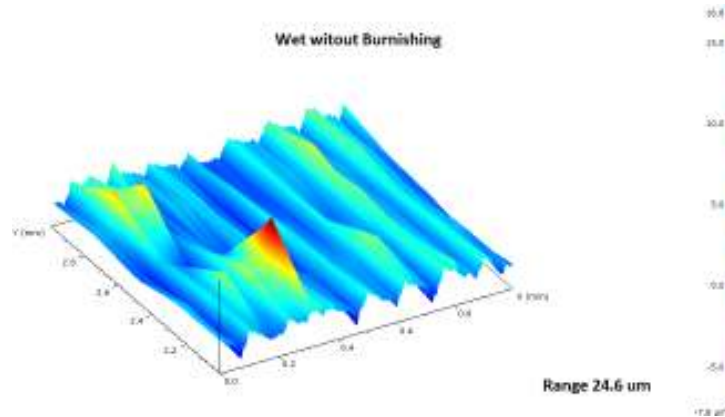


Figure 56 : Surface topography under Wet conditions for RTCE at 5.26 % DCE without burnishing

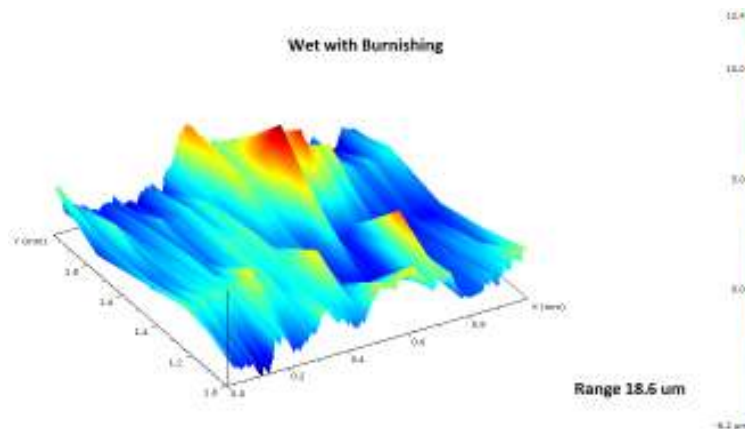


Figure 57 : Surface topography under Wet conditions for RTCE at 5.26 % DCE with burnishing

Serrations, peaks and valleys of large magnitude are found in case of nano RTCE. After the burnishing process, the serrations got removed. However, few peaks and valleys of half the value of the previous magnitude exist as shown in fig. 58. and fig. 59. Maximum improvement in surface topography was found in case of nano RTCE as compared to dry and wet RTCE. Thus the surface roughness of the nano RTCE samples has increased significantly as discussed in the previous section. This finding can clearly be seen in the images shown in fig. 62(e) and fig. 62(f).

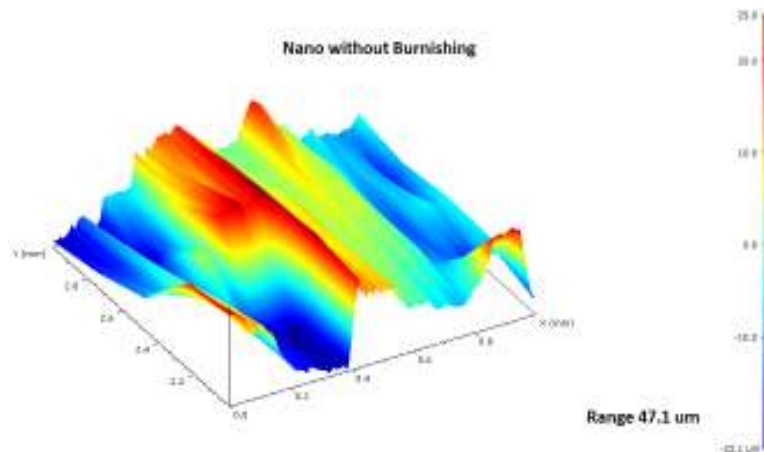


Figure 58 : Surface topography under Nano conditions for RTCE at 5.26% DCE without burnishing

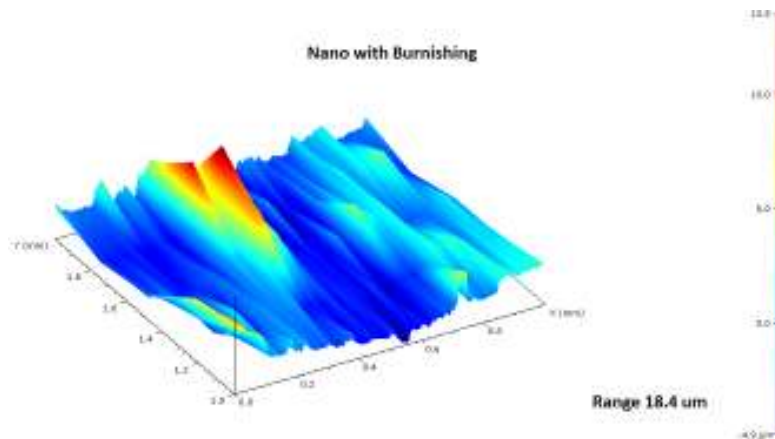


Figure 59 : Surface topography under Nano conditions for RTCE at 5.26 % DCE with burnishing

4.2.4. Ovality

The ovality for the holes with RTCE and RTCE with burnishing is measured. For the measured holes, the diameter of holes for before the burnishing process for all types of RTCE conditions is approximately in the range of 10.02 to 10.03 mm. All samples are burnished to produce hole diameter of approximately 10.3 mm. The ovality measured is shown in fig.60.

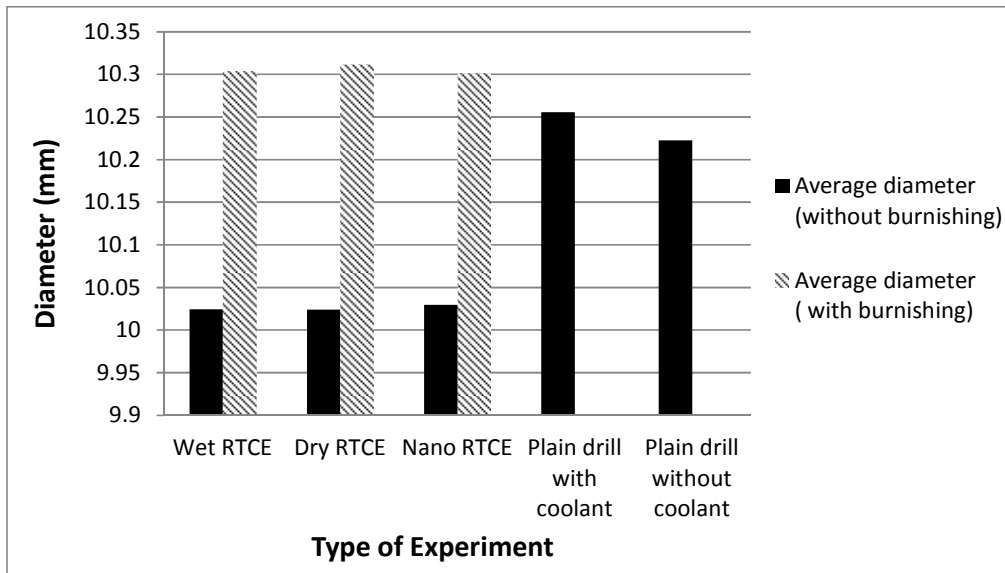


Figure 60 : Ovality measurement for RTCE at 5.26 % DCE

4.2.5. Hardness

The hardness value of samples with hole drilled without coolant and with coolant is 182.47 and 169.69 HRB respectively. The combined cold expansion with burnishing processes resulted in an increase in hardness. The increase in hardness over the samples drilled with coolant is found to be highest, about 39.73 %, in case of RTCE with nanoparticles. This increase in hardness is mainly due to the embedding of nanoparticles over the hole surface. Slight amount of grain refinement also occurs due to the tool stirring action. There is approximately 27.53 % and 20.87 % increase in hardness in case of RTCE under dry and wet conditions respectively. The hardness measured for RTCE and plain drilled samples is shown in fig. 61.

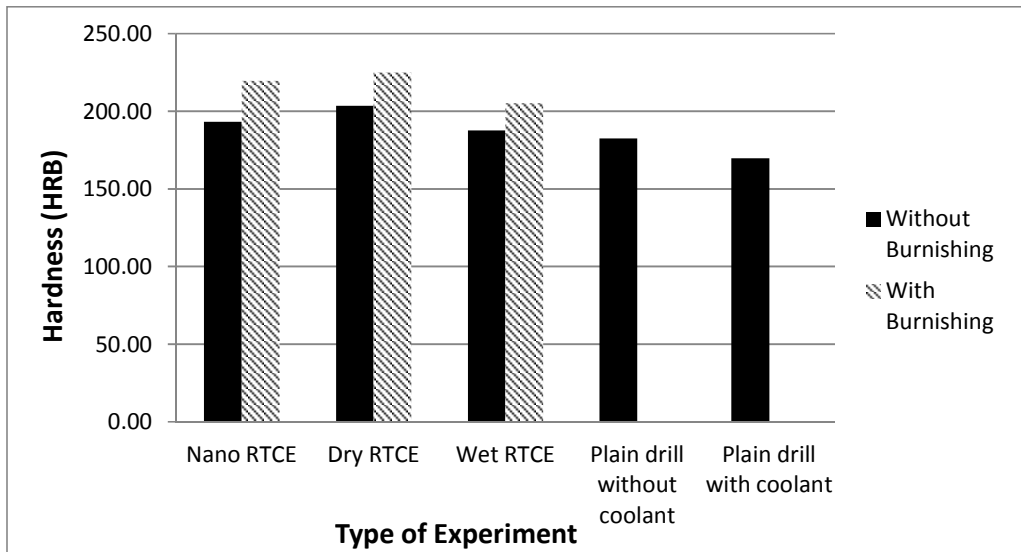
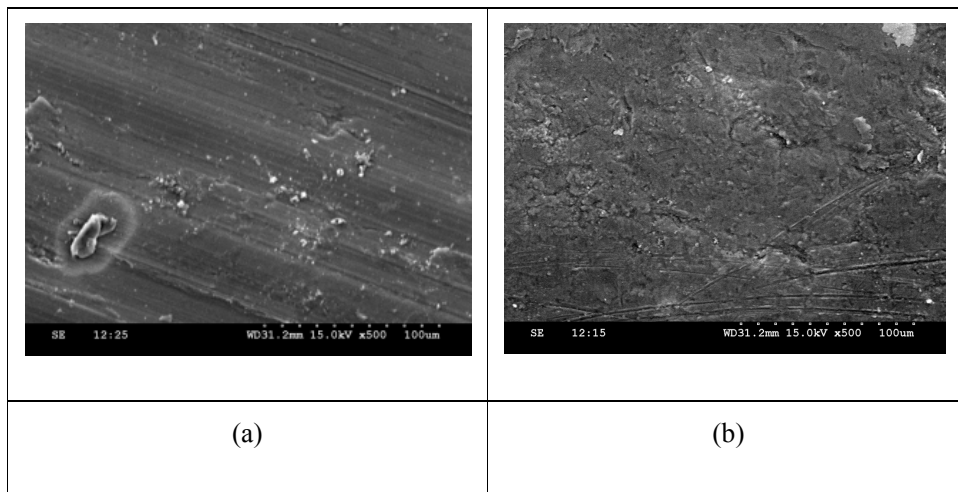


Figure 61 : Hardness measurement for RTCE at 5.26 % DCE

4.2.6. Surface Texture

The RTCE process causes stirring of the material on the surface of the hole. This can be seen by the flow lines created on the surface is shown by the SEM images in fig. 62, fig. 62(a), fig. 62(c) and fig. 62(e) respectively. The pattern of flow appears to be much more prominent after the burnishing process. The burnishing process also reduces the surface irregularities. This effect is demonstrated in fig. 62(b), fig. 62(d) and fig. 62(f) respectively. Higher amount of surface material plastic deformation is observed in case of nanoparticle as compared to wet medium due to the stirring action and additional pressure caused by the presence of nanoparticles. Negligible change in surface is observed in case of CCE (fig.63).



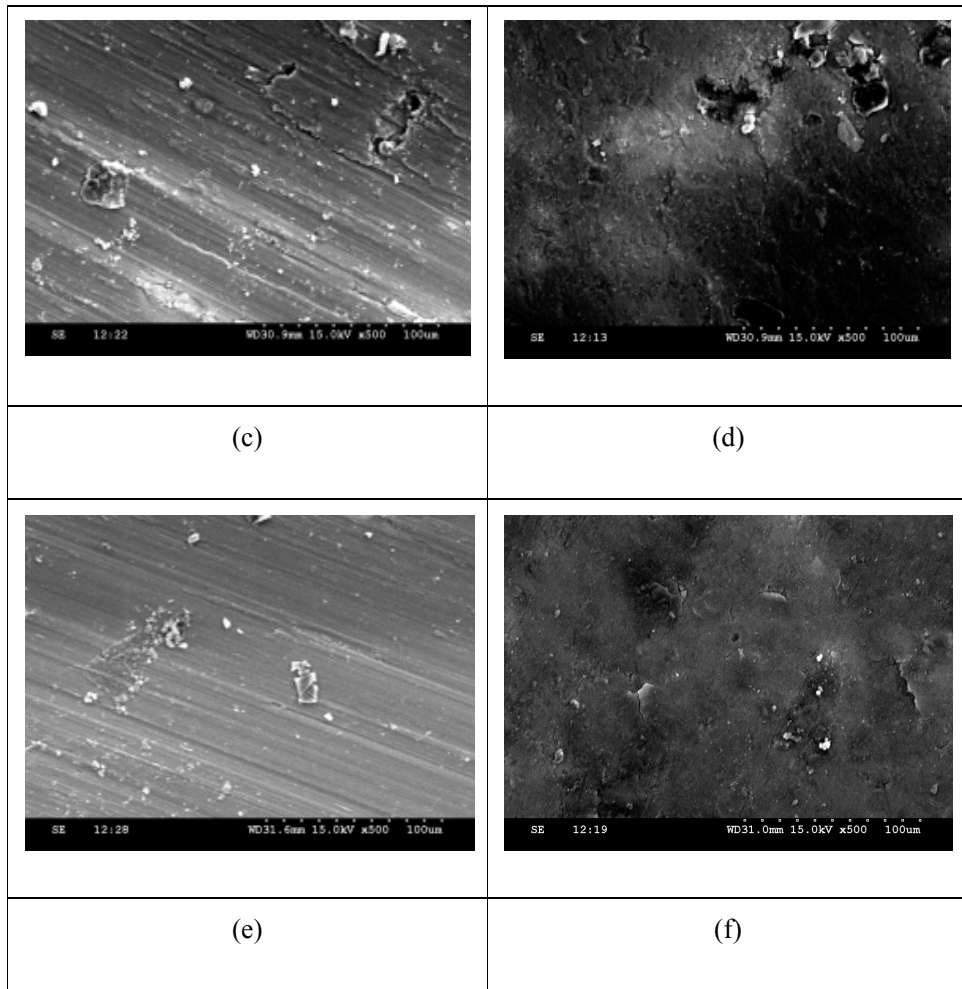


Figure 62 : SEM images showing texture of cylindrical wall for various conditions of (a) Wet RTCE without Burnishing, (b) Wet RTCE With Burnishing, (c) Dry RTCE without Burnishing, (d) Dry RTCE With Burnishing, (e) Nano RTCE without Burnishing, (f) Nano RTCE With Burnishing for Al-2014 T6 material at 5.26% DCE.

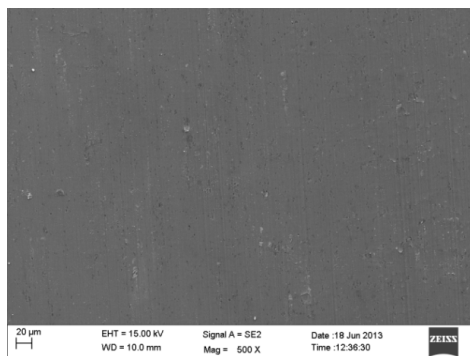


Figure 63 : SEM image showing texture of cylindrical wall for CCE at 5.26% DCE

4.2.7. Fatigue life

The number of cycles to failure of the RTCE specimens without burnishing of the holes and with hole burnishing are presented in table 4 and fig. 64. Fatigue life for RTCE is higher for that of plain drilled sample under all the three conditions. The fatigue life of the samples except for nano RTCE has decreased after the burnishing process. This reason for this decrease in fatigue life may be higher amount of burnishing done. Excessive burnishing may result in sub-surface cracks. This in turn has a detrimental effect on the fatigue life of the sample. In case of nano RTCE, moderate improvement in fatigue life is observed before burnishing with respect to plain drilled hole. However, after the burnishing process, there is approximately 84% increase in fatigue life. It seems that the pressing of nanoparticles on the surface of the hole during the burnishing process has led to embedding of the hard nanoparticles onto the surface of the hole, thereby improving the surface hardness and strength, which in turn has resulted in improved fatigue life. The nanoparticles fill up the cracks on the surface of the hole, also known as mending effect,. During fatigue cycles, the cracks open up during tensile loading. However, during the compression cycle, the nanoparticles arrest the closing of cracks. The loads are applied in the tensile mode only, thereby leading to more fatigue life.

Table 4 : Fatigue life of RTCE operated specimens

RTCE Medium	Fatigue Life Without Burnishing	Fatigue Life With Burnishing
Dry RTCE	69735	58095
Wet RTCE	95924	58396
Nano RTCE	53883	99278

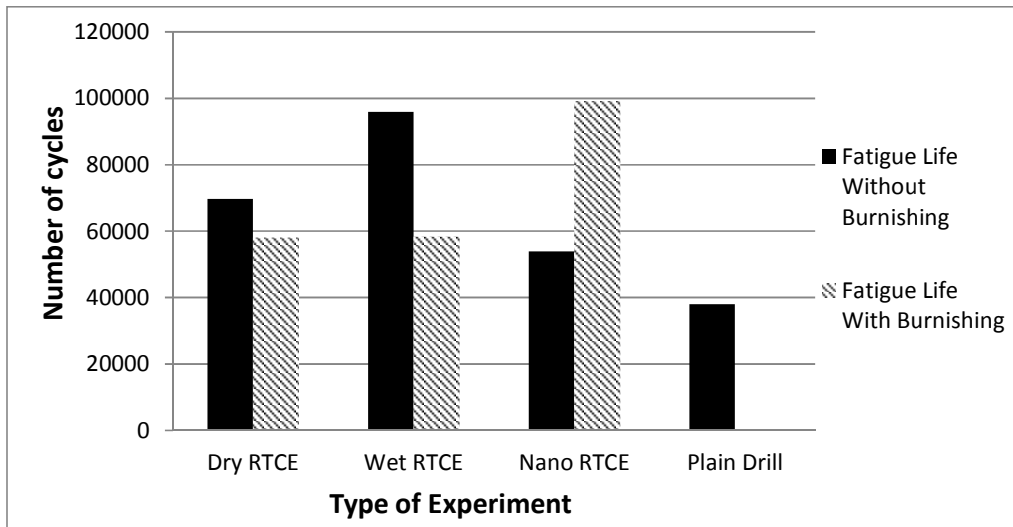


Figure 64 : Fatigue Life for RTCE at 5.26% DCE

4.2.7.1. Effect of residual stress on fatigue life

The fatigue life of RTCE specimens is compared with the induced residual stress as shown in fig. 65. It can be observed that the fatigue life is proportional to residual stress. RTCE under wet condition and nano condition with burnishing shows proportionately higher fatigue life. This can be attributed to the higher surface finish achieved in case of wet samples and nano with burnishing as compared to that achieved in case of RTCE under nano and dry conditions. The plain drilled and nano RTCE without burnishing sample has higher surface roughness due to which the fatigue life achieved for these samples in proportion to the residual stresses is less than expected.

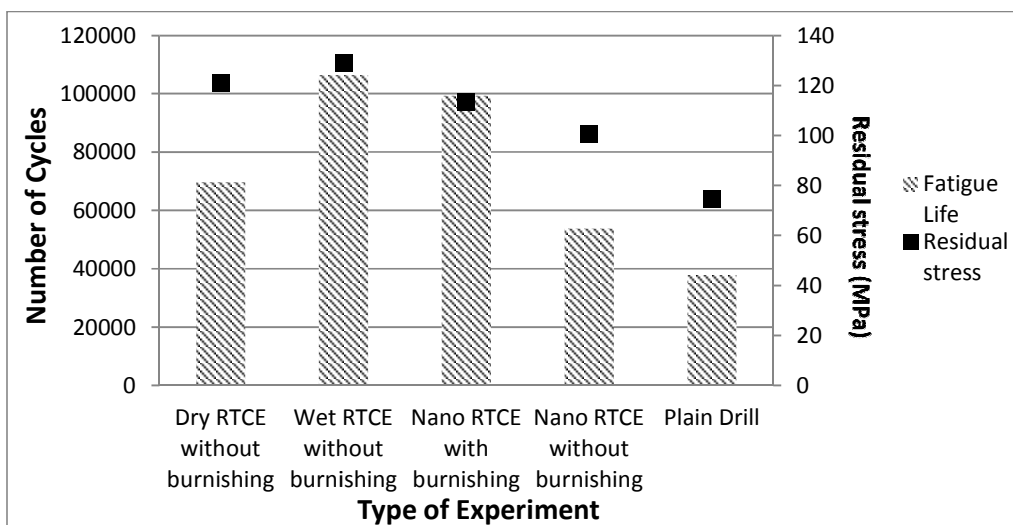


Figure 65 : Comparison of Fatigue life with Residual stress for RTCE at 5.26% DCE

Conventional cold expansion is carried out using the same tapered tool as used for Al specimens. The comparison of fatigue life with residual stress for RTCE and CCE specimens is shown compared to the residual stresses induced. This result for aluminium alloy is in line with those obtained for pure aluminium.in fig. 66. The fatigue life for CCE is proportional to residual stress induced. CCE with 5.26% DCE shows the highest fatigue life as compared to that achieved with 8.69% and 1.01% DCE. Therefore 5.26% is the optimum DCE for 10 mm basic hole size. It is also observed that the CCE at 8.76% DCE results in lower fatigue life as compared to the residual stresses induced. This can be the results of sub-surface cracks due to extreme cold expansion. This result for aluminium alloy is in line with those obtained for pure aluminium.

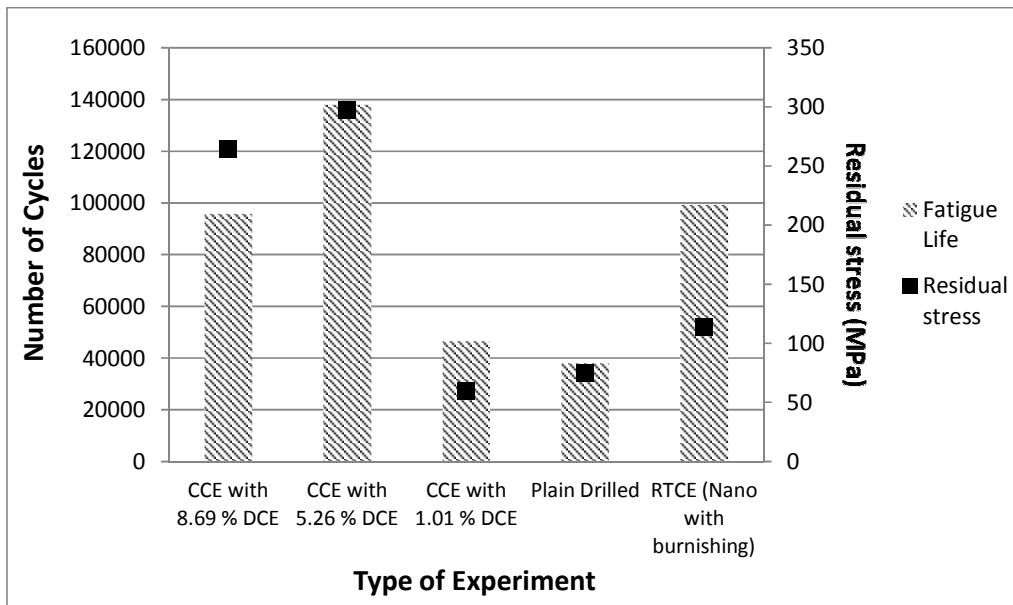


Figure 66 : Fatigue life and Residual stress comparison of RTCE at 5.26% DCE and CCE specimens

4.1.7.2. Effect of surface roughness on fatigue life

Surface roughness is an important factor that can affect crack initiation on the hole surface and thereby lead to fatigue failure. The comparison of fatigue life with surface roughness is shown in fig. 67 to fig. 70. In case of nano RTCE, significant improvement in fatigue life is observed after burnishing. The Ra and Rz values have both reduced post burnishing operation for nano RTCE. These results show that surface roughness is inversely proportional to fatigue life. In case of dry and wet samples, however, although the surface finish has improved after burnishing, the fatigue life has decreased. This may be due to sub-surface cracks occurred due to large amount of burnishing carried out. This effect is not

observed in case of nano RTCE because the fine nanoparticles seemed to act as a powdery lubricant and avoided direct contact of the tool with the hole surface.

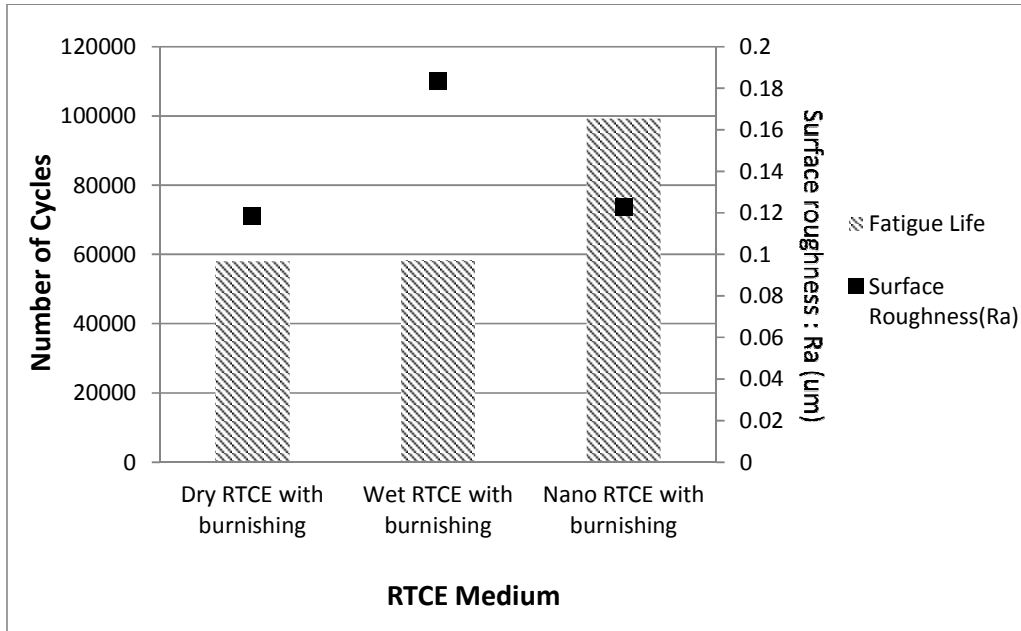


Figure 67 : Fatigue life and Surface roughness (Ra) comparison for RTCE at 5.26% DCE without burnishing

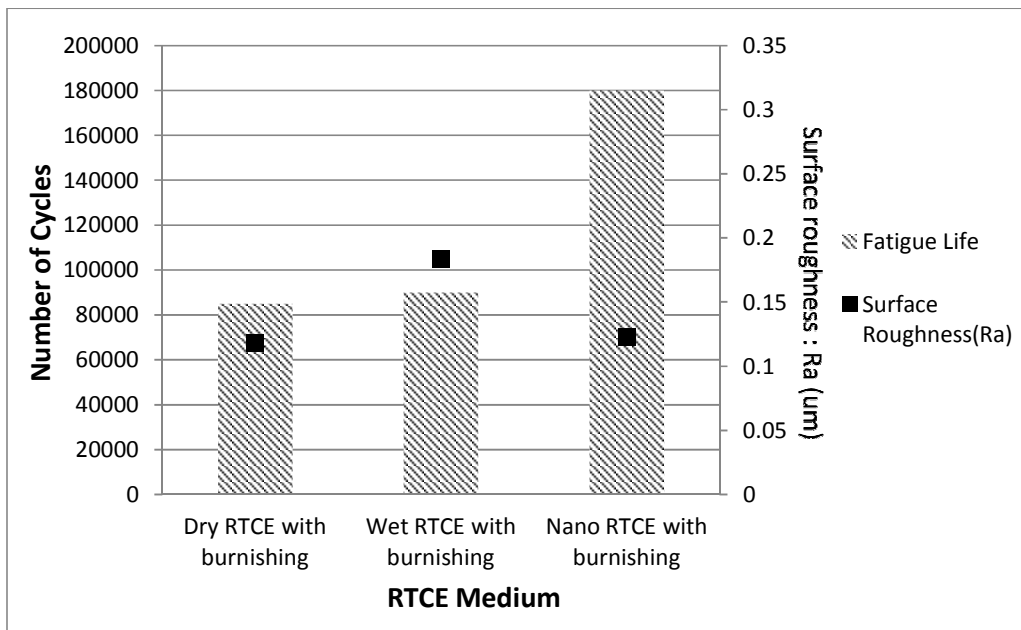


Figure 68 : Fatigue life and Surface roughness (Ra) comparison for RTCE at 5.26% DCE with burnishing

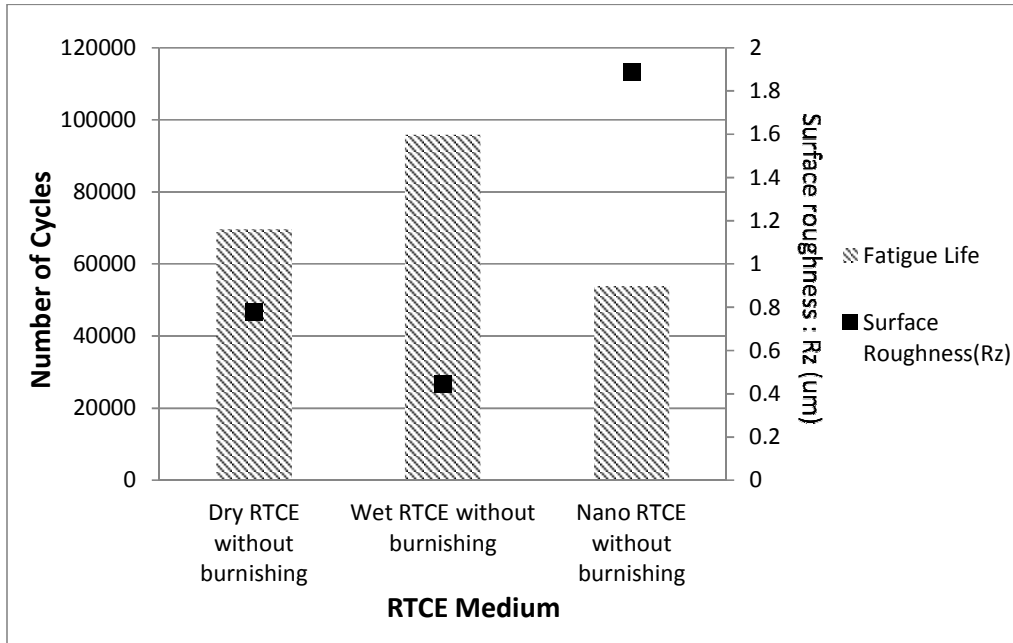


Figure 69 : Fatigue life and Surface roughness (Rz) comparison for RTCE at 5.26% DCE without burnishing

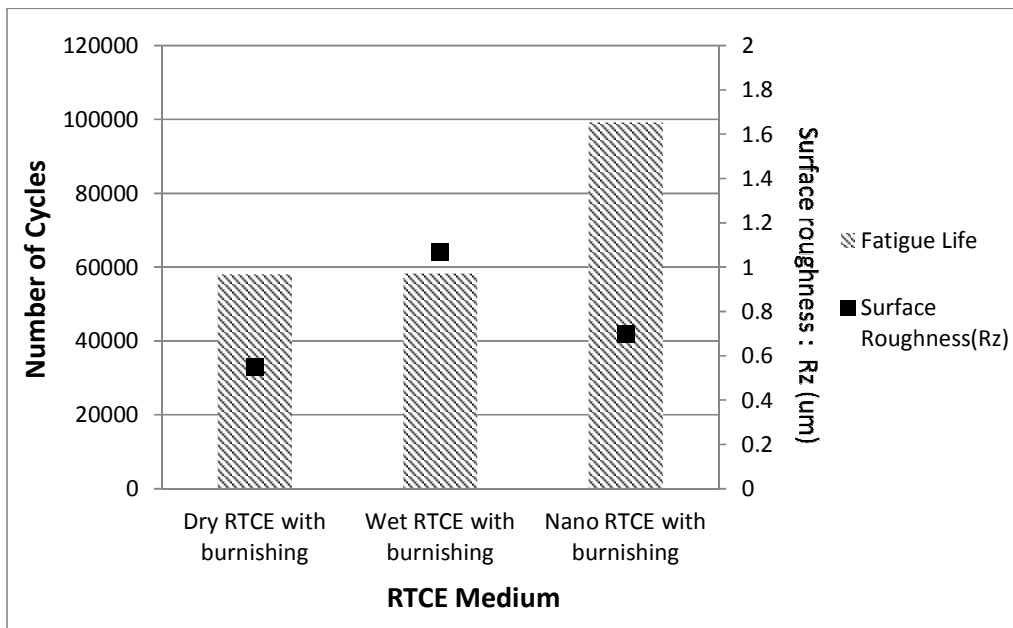


Figure 70 : Fatigue life and Surface roughness (Rz) comparison for RTCE at 5.26% DCE with burnishing

4.1.7.3. Effect of hardness on fatigue life

The comparison of fatigue life with hardness is shown in fig. 71 and fig. 72. It can be observed that in case of dry and wet RTCE, there is an improvement in hardness after the burnishing process. These samples also exhibit a drop in fatigue life. It appears that the increase in hardness increases the brittleness of the hole surface, thereby making it more prone to cracks. Hence, it can be said that hardness has a detrimental effect on the fatigue life of the hole surface. However, in case of nano RTCE, we can observe that there is significant improvement in fatigue life inspite of increase in hardness. The improvement in hardness in case of nano RTCE after burnishing is more likely to be caused by the embedding of nanoparticles. The burnishing tool pressed the nano-particles onto the hole surface which resulted in embedding of nano-particles on the hole surface, thereby improving the surface hardness and strength.

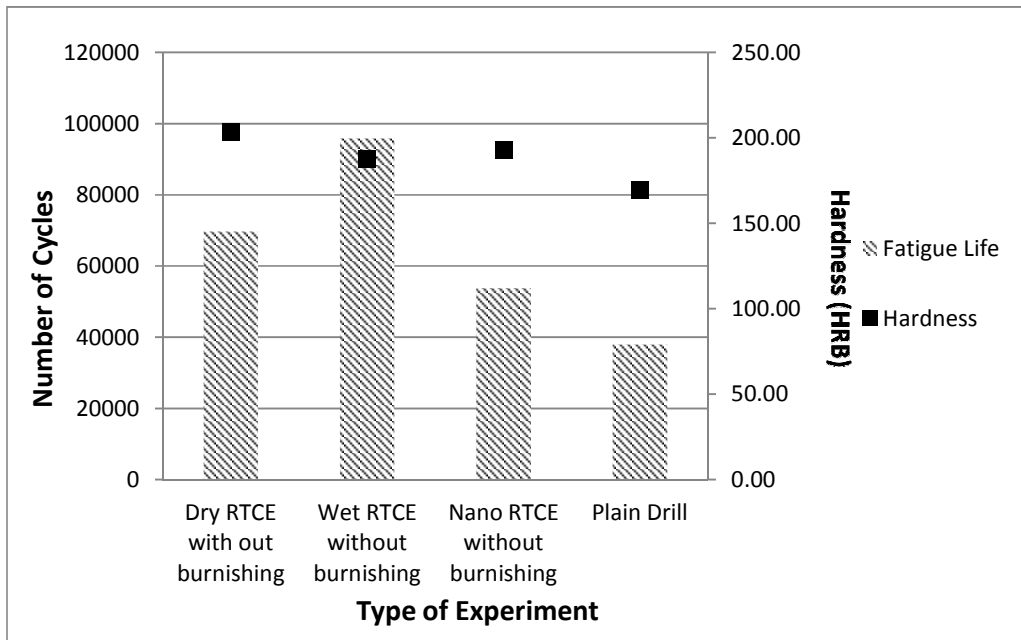


Figure 71 : Fatigue life and hardness comparison of RTCE without burnishing at 5.26% DCE

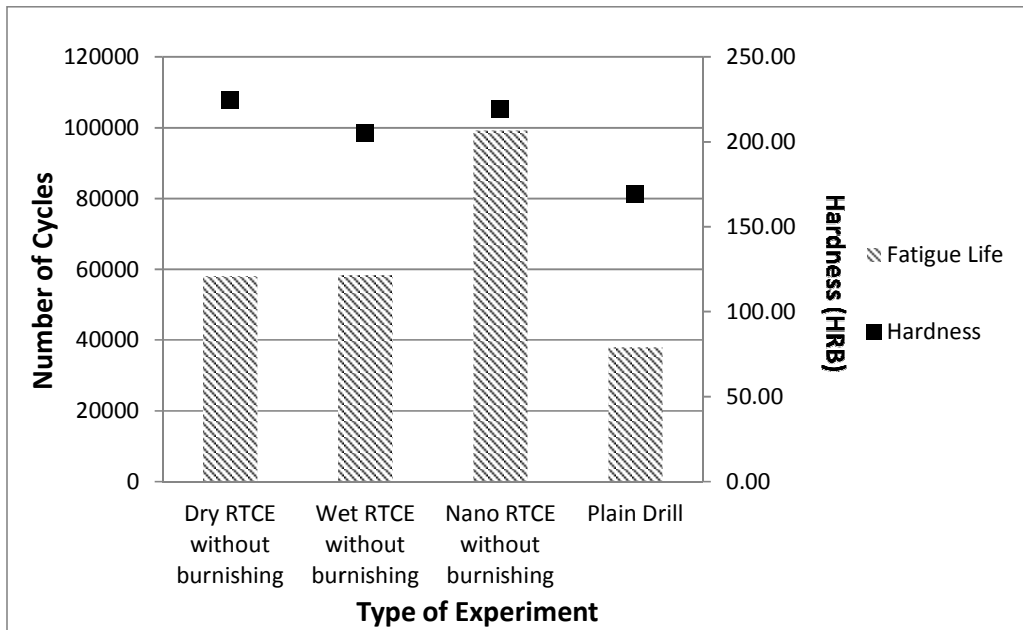


Figure 72 : Fatigue life and hardness comparison of RTCE with burnishing at 5.26% DCE

Chapter 5

Conclusion and Future Work

5.1 Conclusions

1. A novel process is of nanolayering of surface for pure Al and nanolayering with cold expansion is established for Al-2014 T6 Al alloy using a rotating tool. The process is affected by different mediums of cooling and/or lubrication. The process with nanoparticles as medium gives best results for Al and Al-2014 T6 material with respect to hardness, residual stresses induced and fatigue life.
2. The degree of cold expansion (DCE) affects the process. 5.26 % DCE is observed to be the optimum value. The lateral forces acting on the surface of the hole affect RTCE process. Maximum amount of lateral forces are found in nano RTCE at 5.26% DCE.
3. The surface finish of rotating tool cold expanded and burnished cylindrical cavity is improved compared to holes drilled without coolant. Burnishing process improves the surface finish in nano and dry RTCE. The fatigue life is directly proportional to surface finish.
4. There is significant improvement in hardness in case of RTCE with nanoparticles and moderate improvement in hardness is observed in case of dry RTCE for Al material. No significant increase in hardness is found for RTCE under wet conditions. Significant improvement in hardness is found for all three RTCE mediums for Al-2014 T6 material. Hardness had a negative impact on fatigue life, the nano RTCE however is an exception because the hardness improvement has resulted due to embedding of nanoparticles on the hole surface.
5. There is significant improvement in residual stresses induced after the RTCE process for Al-2014 T6 material. Burnishing operation increased it slightly further. Less residual stresses are induced in Al material due to sticking of the material to the tool during the process. The fatigue life is directly proportional to the residual stresses induced.

6. There is significant improvement in the fatigue life of samples after the RTCE process. Maximum efficiency of cold expansion is achieved with nano RTCE with burnishing as compared to conventional cold expansion for Al-2014 T6 material.

5.2 Scope of future work

1. The developed approach can be extended to various aerospace materials and the effect of the RTCE process can be studied further.
2. The variation due to process parameters such as feed rate and rpm needs to be studied further.
3. The variation of the RTCE process due to tool geometry can also be studied.

References

- [1] N. Chandawanich and W. N. Sharpe Jr., “An experimental study of fatigue crack initiation and growth from coldworked holes,” *Engineering Fracture Mechanics*, vol. 11, no. 4, (1979) pp. 609–620.
- [2] M. Heller, R. Jones, and J. F. Williams, “Analysis of cold-expansion for cracked and uncracked fastener holes,” *Engineering Fracture Mechanics*, vol. 39, no. 2, (1991) pp. 195–212.
- [3] P. M. Toor, “Cracks emanating from precracked coldworked holes,” *Engineering Fracture Mechanics*, vol. 8, no. 2, (1976) pp. 391–392.
- [4] M. O. Lai, J. T. Oh, and A. Y. C. Nee, “Fatigue properties of holes with residual stresses,” *Engineering Fracture Mechanics*, vol. 45, no. 5, (Jul. 1993) pp. 551–557.
- [5] P. R. Arora, B. Dattaguru, and H. S. S. Hande, “The fatigue crack growth rate in L-72 Al-alloy plate specimens with cold worked holes,” *Engineering Fracture Mechanics*, vol. 42, no. 6, (Aug. 1992) pp. 989–1000.
- [6] Galip Keçelioglu, “Stress and fracture analysis of riveted joints,” Middle East Technical University, 2008.
- [7] Y. Liu, J. Liu, and X.-J. Shao, “Study on the Residual Stress Fields, Surface Quality, and Fatigue Performance of Cold Expansion Hole,” *Materials and Manufacturing Processes*, vol. 26, no. 2, (2011) pp. 294–303.
- [8] A. Amrouche, M. Su, A. Aid, and G. Mesmacque, “Numerical study of the optimum degree of cold expansion: Application for the pre-cracked specimen with the expanded hole at the crack tip,” *Journal of Materials Processing Technology*, vol. 197, no. 1–3, (Feb. 2008) pp. 250–254.
- [9] H. D. Gopalakrishna, H. N. Narasimha Murthy, M. Krishna, M. S. Vinod, and A. V. Suresh, “Cold expansion of holes and resulting fatigue life enhancement and residual stresses in Al 2024 T3 alloy – An experimental study,” *Engineering Failure Analysis*, vol. 17, no. 2, (Mar. 2010) pp. 361–368.

- [10] K. Farhangdoost and A. Hosseini, "The Effect of Mandrel Speed upon the Residual Stress Distribution around Cold Expanded Hole," *Procedia Engineering*, vol. 10, no. 0, (2011) pp. 2184–2189.
- [11] T. N. Chakherlou and J. Vogwell, "The effect of cold expansion on improving the fatigue life of fastener holes," *Engineering Failure Analysis*, vol. 10, no. 1, (Feb. 2003) pp. 13–24.
- [12] T. N. Chakherlou, M. Shakouri, A. B. Aghdam, and A. Akbari, "Effect of cold expansion on the fatigue life of Al 2024-T3 in double shear lap joints: Experimental and numerical investigations," *Materials & Design*, vol. 33, no. 0, (Jan. 2012) pp. 185–196.
- [13] J. Liu, X. J. Shao, Y. S. Liu, and Z. F. Yue, "Effect of cold expansion on fatigue performance of open holes," *Materials Science and Engineering: A*, vol. 477, no. 1–2, (Mar. 2008) pp. 271–276.
- [14] L. Yongshou, S. Xiaojun, L. Jun, and Y. Zhufeng, "Finite element method and experimental investigation on the residual stress fields and fatigue performance of cold expansion hole," *Materials & Design*, vol. 31, no. 3, (Mar. 2010) pp. 1208–1215.
- [15] M. Burlat, D. Julien, M. Lévesque, T. Bui-Quoc, and M. Bernard, "Effect of local cold working on the fatigue life of 7475-T7351 aluminium alloy hole specimens," *Engineering Fracture Mechanics*, vol. 75, no. 8, (May 2008) pp. 2042–2061.
- [16] W. Z. Yan, X. S. Wang, H. S. Gao, and Z. F. Yue, "Effect of split sleeve cold expansion on cracking behaviors of titanium alloy TC4 holes," *Engineering Fracture Mechanics*, vol. 88, no. 0, (Jul. 2012) pp. 79–89.
- [17] P. M. G. P. M. P. F.P. de Matos, "Reconstitution of fatigue crack growth in Al-alloy 2024-T3 open-hole specimens using microfractographic techniques," *Engineering Fracture Mechanics*, no. 14, (2005) pp. 2232–2246.
- [18] A. T. Özdemir and R. Hermann, "Effect of expansion technique and plate thickness on near-hole residual stresses and fatigue life of cold expanded holes," *Journal of Materials Science*, vol. 34, no. 6, (Mar. 1999) pp. 1243–1252.
- [19] A. H. Shamdani and S. Khoddam, "A comparative numerical study of combined cold expansion and local torsion on fastener holes," *Fatigue & Fracture of Engineering Materials & Structures*, vol. 35, no. 10, (2012) pp. 918–928.

[20] J. T. Maximov and G. V. Duncheva, "A new 3D finite element model of the spherical mandrelling process," *Finite Elements in Analysis and Design*, vol. 44, no. 6–7, (Apr. 2008) pp. 372–382.

[21] Lee, K., Hwang, Y., Cheong, S., Choi, Y., Kwon, L., Lee, J., Kim, S.H., 'Understanding the Role of Nanoparticles in Nano-oil Lubrication. *Tribol Lett* 35, (2009) 127–131.

Appendix

Force data for Conventional Cold Expansion

Aluminium

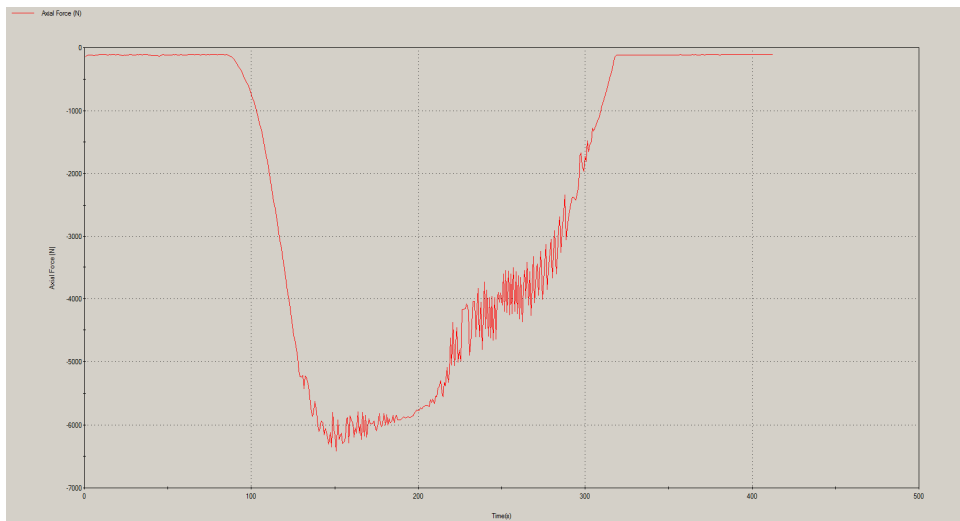


Figure 1 : Force for 8.76 % DCE (Fz)

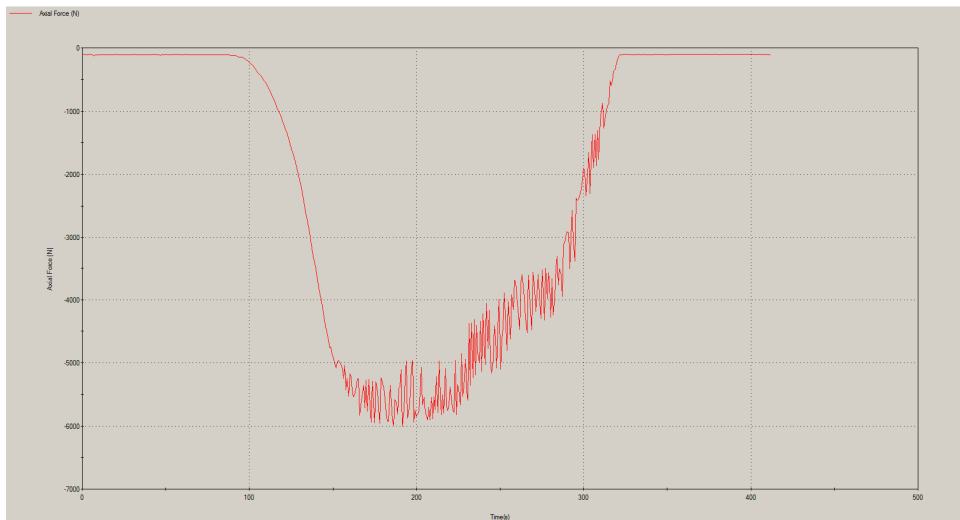


Figure 2 : Force for 5.26 % DCE (Fz)

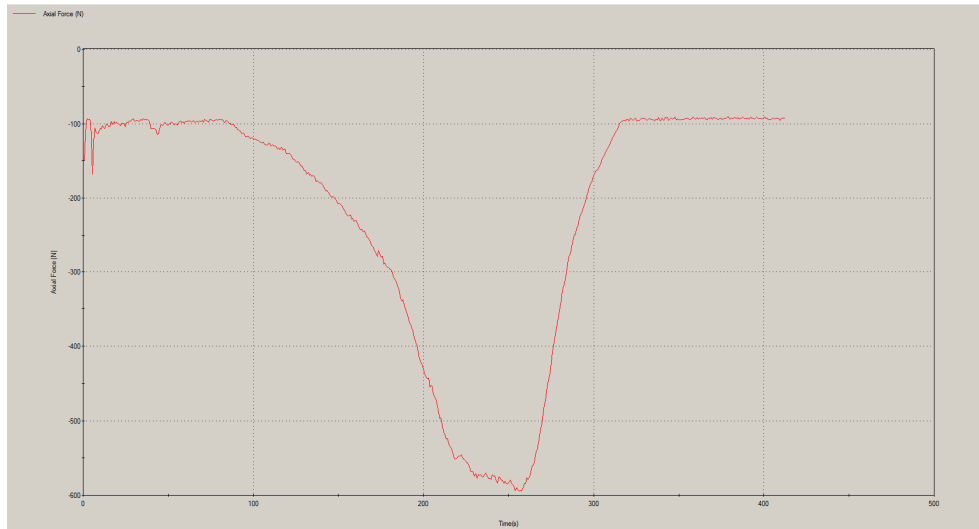


Figure 3 : Force for 1.01 % DCE (Fz)

Aluminium alloy : Al 2014-T6

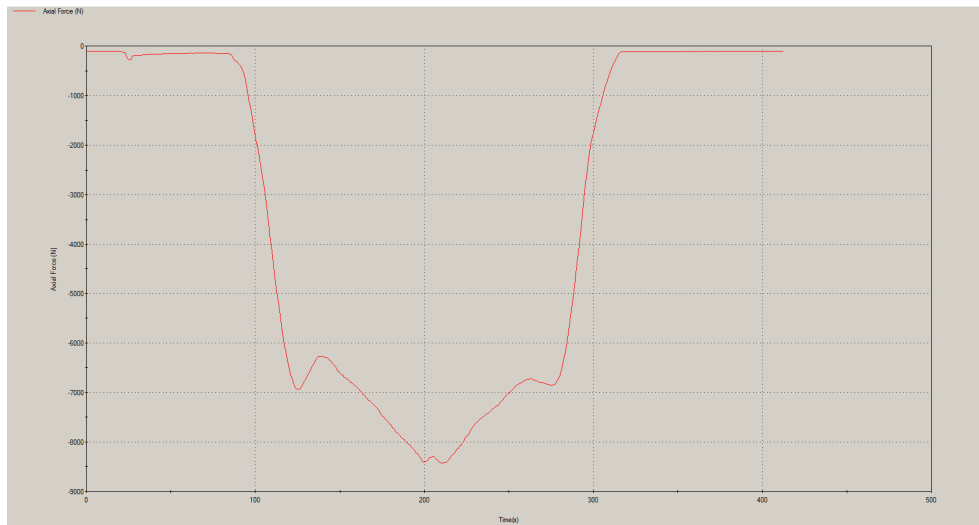


Figure 4 : Force for 8.76 % DCE (Fz)

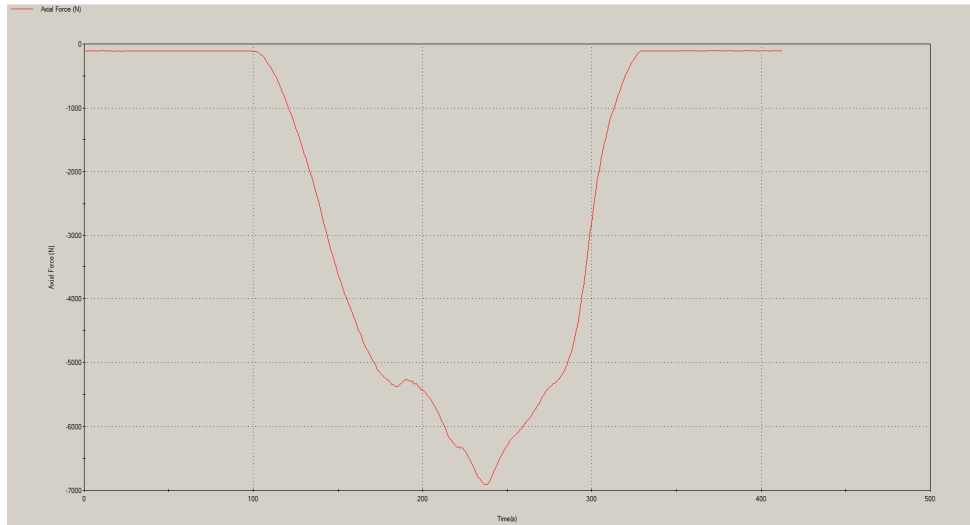


Figure 5 : Force for 5.26 % DCE (Fz)

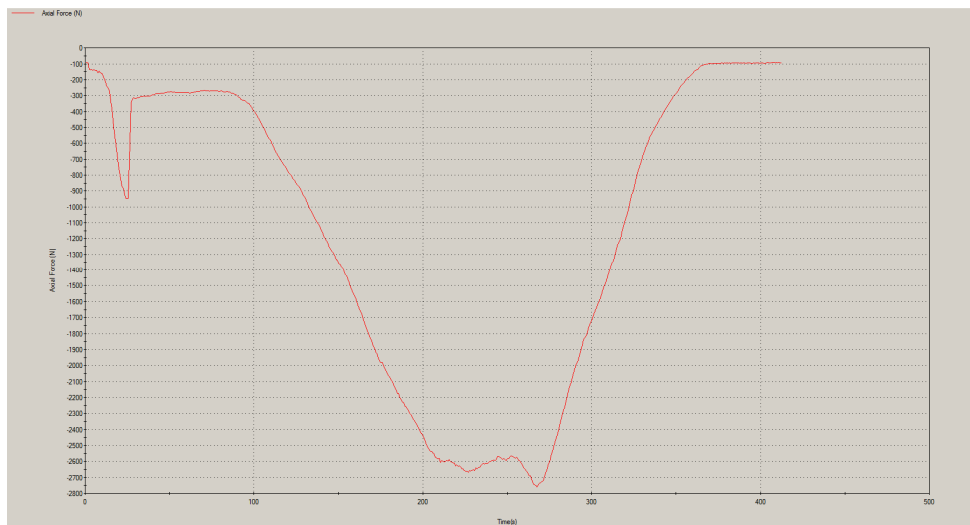


Figure 6 : Force for 1.01 % DCE (Fz)